Cancer Chemother Pharmacol (2012) 69:229–237
DOI 10.1007/s00280-011-1687-8

ORIGINAL ARTICLE

# Pharmacokinetic characterization of a natural product–inspired novel MEK1 inhibitor E6201 in preclinical species

**Vipul Kumar · Edgar L. Schuck · Robert D. Pelletier · Nadia Farah · Krista B. Condon · Meng Ye · Christopher Rowbottom · Belinda M. King · Zhi-Yi Zhang · Philip L. Saxton · Y. Nancy Wong**

Received: 10 March 2011 / Accepted: 31 May 2011 / Published online: 23 June 2011


**Abstract**
*Purpose* E6201 is a natural product–inspired novel inhibitor of mitogen-activated protein kinase/extracellular signal–regulated kinase kinase-1 (MEK1) and other kinases and is currently under development as an anticancer (parenteral administration) and antipsoriasis agent (topical application). In vitro and in vivo preclinical studies were performed to characterize the pharmacokinetics of E6201. Allometric scaling was applied to predict human pharmacokinetics of E6201.
*Methods* In vitro metabolism studies for CYP induction and CYP inhibition were conducted using human hepatocytes and microsomes, respectively. Metabolic stability using microsomes and protein-binding studies using pooled plasma were performed for mice, rats, dogs, and human. Pharmacokinetics of E6201 and its isomeric metabolite, ER-813010, in mice, rats, and dogs was determined following single IV administration of E6201 at three dose levels. Bioanalysis was performed using LC/MS/MS. Pharmacokinetic parameters were determined using non-compartmental analysis, and allometric scaling with a two-compartment model was used to predict E6201 pharmacokinetics in humans.
*Results* E6201 showed high plasma protein binding (>95%), and metabolic stability half-life ranged from 36 to 89 min across species. In vitro CYP inhibition (CYP1A2, 2C9, 2C19, 2D6, 2E1, and 3A) and CYP induction (CYP1A, 3A, 2C9, and 2C19) suggested no inhibitory or induction effect on the tested human CYPs up to 10 μM of E6201. Pharmacokinetics of E6201 in mice, rats, and dogs was characterized by mean clearance ranging from 3.45 to 10.92 L/h/kg, distribution volume ranging from 0.63 to 13.09 L/kg, and elimination half-life ranging from 0.4 to 1.6 h. ER-813010 was detected in all species with metabolite to parent exposure ratio ($AUC_R$) ranging from 3.1 to 33.4% and exhibited fast elimination (<3 h). The allometry predicted high clearance and large volume of distribution of E6201 in humans and was in general in good agreement with the observed first human subject pharmacokinetics.
*Conclusions* E6201 exhibited high clearance, high to moderate distribution, and fast elimination in preclinical species. In vitro results suggested that E6201 has low risk of drug–drug interactions due to CYP inhibition and induction in humans. In the first-in-man study, E6201 exhibited high clearance, which was well predicted by allometric scaling.

**Keywords** E6201 · Pharmacokinetics · MEK1 inhibitor · Protein binding · CYP induction · CYP inhibition

Part of this work was presented at the 38th American college of clinical pharmacology annual meeting 2009, San Antonio, TX, USA (Abstract No. 142).

*Present Address:*
V. Kumar (✉)
Non-clinical Drug Development, Cubist Pharmaceuticals,
65 Hayden Avenue, Lexington, MA 02421, USA
e-mail: vipul686@yahoo.com

E. L. Schuck · R. D. Pelletier · N. Farah ·
K. B. Condon · M. Ye · C. Rowbottom ·
P. L. Saxton · Y. N. Wong
DMPK-Andover, Biopharmaceutical Assessments CFU,
Eisai Inc., Andover, MA 01810, USA

B. M. King
Development Quality Assurance,
Eisai Inc., Andover, MA 01810, USA

*Present Address:*
Z.-Y. Zhang
Department of Drug Metabolism and Pharmacokinetics,
Biogen Idec, 14 Cambridge Center,
Cambridge, MA 02142, USA

## Introduction

E6201, a totally synthetic analog of LL-Z1640-2 (in the zearelenone natural product family, [3]), is a novel inhibitor of mitogen-activated protein kinase/extracellular signal–regulated kinase kinase-1 (MEK1) and other kinases [11, 14]. It was found to be effective as an anti-inflammatory and antihyperproliferative agent both in vitro and in vivo [5]. It suppressed cancer cell growth with $IC_{50}$ values in low nanomolar (nM) range [11, 14]. The chemical structures of E6201 and its isomeric metabolite, ER-813010, are shown in Fig. 1. Currently, E6201 is under development as an anticancer (parenteral administration) and antipsoriasis agent (topical application).

In cancer, the RAS/RAF/MEK/ERK signaling pathway has been viewed as a pathway to target for developing novel anticancer therapies, based on its central role in regulating growth and survival of cells in a broad spectrum of human cancers [15, 16]. Importantly, mitogen-activated protein kinase/extracellular signal–regulated kinase kinase-1 (MEK1) is downstream of RAS and RAF proteins, which are often mutated [2] and abnormally active in tumors. Therefore, MEK1 inhibition is an attractive target for anticancer therapy. A series of in vivo xenograft animal studies have demonstrated antitumor activity of E6201 with potent activity against V600E BRAF-mutated human cancer xenografts [11, 18] prompting us to further develop E6201.

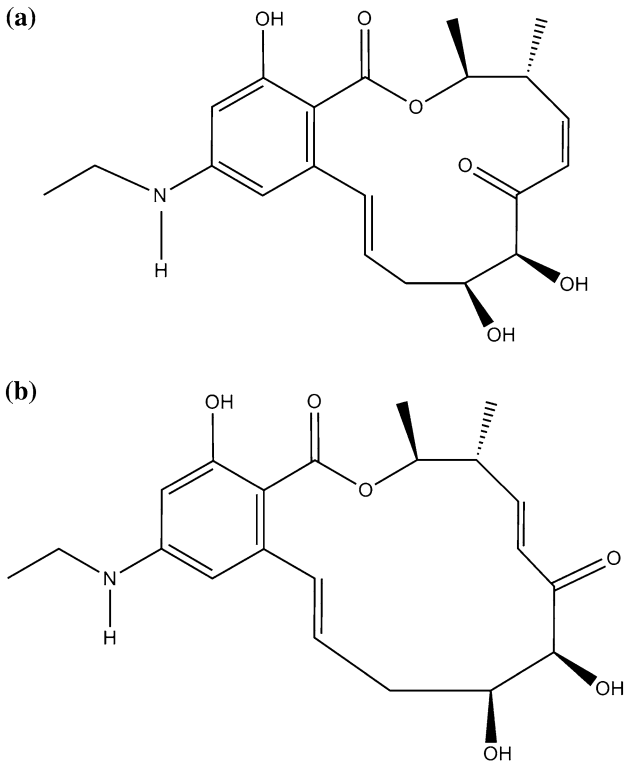


**Fig. 1** Chemical structure of (**a**) E6201 and (**b**) isomeric metabolite, ER-813010

Preclinical pharmacokinetics and metabolism characterization of a potential candidate compound is an integral part of drug discovery and development [8]. This manuscript describes the preclinical pharmacokinetic characterization of E6201 in mice, rats, and dogs. In vitro metabolism and plasma protein-binding studies of E6201 are also described. Utilizing the preclinical data, allometric scaling was applied to predict human pharmacokinetics of E6201.

## Materials and methods

### Materials

E6201 and its isomeric metabolite, ER-813010, were synthesized by the Pharmaceutical Science and Technology Core Function Unit (CFU) of Eisai Inc. (Andover, MA, USA). Blank mouse, rat, and dog plasma were purchased from Bioreclamation Inc. (Westbury, NY, USA), and blank human plasma was purchased from Biological Specialty Corporation (Colmar, PA, USA). Pooled mouse, rat, dog, and human liver microsomes were purchased from BD Biosciences (Woburn, MA, USA). Monohydroxylated warfarin metabolites (6- and 7-hydroxywarfarin), (±)-bufuralol, (±)-1′-hydroxybufuralol, chlorzoxazone, 6-hydroxychlorzoxazone, (±)-4′-hydroxymephenytoin, 1′- and 4-hydroxymidazolam were purchased from BD Biosciences. Albendazole, allyl sulfide, α-naphthoflavone, ketoconazole, magnesium chloride, mebendazole, midazolam, niflumic acid, NADPH, R-propranolol, quinidine, sulfaphenazole, tranylcypromine, triazolam, TRIZMA, and racemic-warfarin were obtained from Sigma Chemical Corp. (St. Louis, MO, USA). S-Mephenytoin was purchased from BIOMOL Research Laboratories Inc. (Plymouth Meeting, PA, USA). Optically pure R- and S-warfarin were prepared from racemic mixtures by a differential crystallization method (enantiomer purity ≥98%). All chemicals, reagents, and solvents used were of either analytical or HPLC grade. Millipore water (Millipore Corporation, Billerica, MA, USA) was used in all experiments.

### In vitro plasma protein binding

The in vitro plasma protein binding of E6201 in mouse, rat, dog, and human plasma ($n = 3$ per concentration per species) was determined using equilibrium dialysis. The binding was determined at 100, 500, 1,000, 3,000, 10,000, and 30,000 ng/mL of E6201. The spiked plasma was placed on one side of the membrane with phosphate-buffered saline on the other side. The system was incubated

at approximately 37°C on an orbital shaker for 4 h. Aliquots from plasma and buffer chambers were collected, appropriately labeled, extracted and were analyzed using LC/MS/MS.

### In vitro metabolic stability, CYP inhibition and CYP induction studies

The in vitro stability of E6201 was investigated in incubations with liver microsomal fractions from mouse, rat, dog, and human. The half-life ($t_{1/2}$) of E6201 depletion ($n = 3$) was determined under the following final conditions: E6201 (5 μM); microsomes (2 mg/mL); in pH 7.4 Tris buffer (50 mM) containing 15 mM magnesium chloride. Incubations were performed in test tubes at approximately 37°C. Incubations were initiated by the addition of NADPH and were quenched at various time points (0, 5, 15, 30, 45, 60, or 120 min) by the addition of an equal volume (0.25 mL) of methanol. The supernatants were analyzed using LC/MS/MS.

The inhibition potential of E6201 on CYP1A2, 2C9, 2C19, 2D6, 2E1, and 3A activities was assessed using pooled human liver microsomes. The effect of E6201 on the metabolic rates of CYP-specific probe reactions was measured in triplicate under the following final conditions: E6201 (1, 5, or 10 μM); microsomes (2 mg/mL); R-warfarin (2 mM); S-warfarin (200 μM); S-mephenytoin (200 μM); bufuralol (4 μM); chlorzoxazone (200 μM); midazolam (40 μM); in pH 7.4 Tris buffer (50 mM) containing 15 mM magnesium chloride. CYP-selective inhibitors (α-naphthoflavone, tranylcypromine, sulfaphenazole, quinidine, allyl sulfide, and ketoconazole) served as positive controls. Incubations were performed in test tubes at approximately 37°C. Incubations were initiated by the addition of NADPH and were quenched at respective times (10 min for CYP3A-mediated midazolam 1′-and 4-hydroxylations, 15 min for CYP2D6-mediated bufuralol 1′-hydroxylation, 30 min for CYP2E1-mediated chlorzoxazone 6-hydroxylation, 60 min for CYP1A2-mediated R-warfarin 6-hydroxylation, CYP2C9-mediated S-warfarin 7-hydroxylation and CYP2C19-mediated S-mephenytoin 4′-hydroxylation) by the addition of an equal volume (0.25 mL) of methanol. The supernatants were analyzed using LC/MS/MS.

Primary human hepatocytes were used to evaluate the potential of E6201 to induce CYPs at 1, 5, or 10 μM concentrations of E6201. Potential inductions of CYP1A2, 3A, 2C9, and 2C19 were assessed using CYP form-specific metabolism activities determined by LC/MS/MS and by Western immunoblotting using anti-human CYP antibodies [6, 9, 17]. The positive controls for induction were 2,3,7,8-tetrachlorodibenzo-*p*-dioxin (TCDD; 20 nM) for CYP1A and rifampicin (10-50 μM) for CYP2C and CYP3A [12, 13, 19]. Methanol was used as the vehicle (negative) control. The treatment period was 72 h with media, treatment replacement occurring every 24 h.

### Pharmacokinetic experiments

Pharmacokinetic studies were performed in accordance with the Institutional Animal Care and Use Committee (IACUC) of Eisai (for mouse and rat studies) or IACUC, or equivalent committee, of the Contract Research Organisation (CRO) for the dog study.

#### Mouse

Male BALB/c mice (Charles River Laboratories, Kingston, NY, USA) weighing 22–24 g at the start of the study were administered 1, 5, and 10 mg/kg of E6201 IV (20% (w/v) hydroxypropyl-β-cyclodextrin solution) via tail vein injection ($n = 3$/time point/dose group) at 10 mL/kg dosing volume. Blood samples were collected by cardiac puncture at 5, 15, 30 min, 1, 2, 4, 6, and 8 h postdose with EDTA as the anticoagulant and placed on ice. Harvested plasma samples were appropriately labeled and stored at approximately −20°C pending LC/MS/MS analysis.

#### Rat

Male Sprague–Dawley rats (Hilltop, Scottdale, PA, USA), weighing 226–250 g at the start of the study, were administered 1, 5, and 10 mg/kg of E6201 IV via tail vein injection ($n = 3$/dose group). The rats were jugular vein cannulated to facilitate multiple sampling from a single animal. The formulation and dosing volume for rat were identical to that of mouse study. Blood samples were collected at 5, 15, 30 min, 1, 2, 4, 6, and 8 h postdose with EDTA as the anticoagulant and placed on ice. Harvested plasma samples were appropriately labeled and stored at approximately −20°C pending LC/MS/MS analysis.

#### Dog

Four male beagle dogs (Marshall Farms; North Rose, NY, USA) weighing 8–10 kg at the start of the study, each identified by a numbered ear tattoo, were administered E6201 at 0.5, 1.5, and 5 mg/kg IV in a dose-escalating crossover design with a 1-week washout between doses. E6201 was dissolved in a 20% (w/v) hydroxypropyl-β-cyclodextrin solution and administered at the dosing volume of 5 mL/kg. The IV doses were administered through an indwelling catheter, inserted into a cephalic or

saphenous vein, as a short infusion over a period of 5 min. Blood samples were collected from the jugular vein at predose, 5, 15, 30 min, 1, 2, 4, 6, 8, 12, and 24 h postdose with sodium heparin as the anticoagulant and placed on ice. Harvested plasma samples were appropriately labeled and stored at approximately −70°C pending LC/MS/MS analysis.

## Bioanalysis

Samples obtained from the pharmacokinetic studies were assayed for E6201 and its isomeric metabolite, ER-813010, concentration using LC/MS/MS. A structurally similar analog was used as an internal standard (IS, Eisai proprietary compound) for sample analysis. For pharmacokinetic samples, plasma was mixed with IS and diluted with 500 μL of water. The samples were then extracted by liquid–liquid extraction using 5 mL of ethyl acetate. The organic phase was separated and dried under nitrogen. The samples were reconstituted in 200 μL of methanol/water (50/50) solution and injected onto the LC/MS/MS. The protein-binding samples (100 μL) were processed by protein precipitation with 200 μL of methanol containing IS solution and the clear supernatant was injected onto the LC/MS/MS. The HPLC systems consisted of either a Waters 2695 Separations Module system (Milford, MA), an Agilent HPLC (Agilent Technologies, Santa Clara, CA), or a Shimadzu HPLC system (Shimadzu Scientific Instruments, Columbia, MD). Samples were injected on a C18 Waters YMC$^{TM}$ ODS-AM (23 × 2.0 mm) column maintained at approximately 25°C at a flow rate of 0.3 mL/min with a gradient elution. Samples were injected using the autosampler maintained at approximately 4°C. The mobile phase consisted of 0.1% (v/v) formic acid in water (A) and 0.1% (v/v) formic acid in methanol (B). The initial mobile phase composition was 65% A/35% B and was changed to 100% B over 5 min and held constant for an additional 2 min postinjection. The mobile phase composition then returned to initial conditions with 2.9 min for column re-equilibration with a total analysis time of 10 min. The HPLC was interfaced to a Micromass Quattro Ultima (Micromass Limited, Beverly, MA) or an AB Sciex API2000/API4000 (Foster City, CA) triple quadrupole mass spectrometer using electrospray ionization under positive ion mode. Data acquisition utilized multiple reaction monitoring (MRM). E6201 and ER-813010 were monitored at precursor ion m/z 390.2 and product ion m/z 232.0, and the IS was monitored at precursor ion m/z 450.2 and product ion m/z 274.0. The retention times for E6201, ER-813010, and IS were approximately 5.6, 5.2, and 5.6 min, respectively. Quantitation was based on a linear regression with a $1/x^2$ weighting factor of the peak area ratios of E6201 to IS or ER-813010 to IS versus concentration.

## Pharmacokinetic data analysis and allometric scaling

The plasma concentration versus time data of E6201 and ER-813010 following E6201 IV administration was analyzed using non-compartmental approach (WinNonlin v. 4.0.1 [Pharsight; Mountain View, CA, USA]). The area under the curve (AUC) from time zero to the last quantifiable time point postdose ($AUC_{0-t}$) was calculated using the trapezoidal method. The $AUC_{0-\infty}$ was calculated as $AUC_{0-t} + AUC_{extrap}$, where $AUC_{extrap}$ represents the extrapolated AUC from the last quantifiable time point ($C_{last}$) to infinity and was calculated as $C_{last}/\lambda_z$. Lambda z ($\lambda_z$), the slope of the concentration versus time curve during the terminal phase, was determined by linear regression and used for determining the elimination half-life ($t_{1/2}$) as $\ln 2/\lambda_z$. The observed area under the first-moment plasma concentration versus time curve ($AUMC_{0-t}$) was calculated by the trapezoidal rule, while the estimated area under the first-moment plasma concentration versus time curve from time zero to infinity ($AUMC_{0-\infty}$) was calculated as:

$$AUMC_{0-\infty} = AUMC_{0-t} + \frac{C_{last} \cdot t_{last}}{\lambda_z} + \frac{C_{last}}{\lambda_z^2}$$

The total body clearance (CL) and the volume of distribution at steady state ($V_{ss}$) were calculated as dose/$AUC_{0-\infty}$ and $CL \cdot MRT_{0-\infty}$, respectively. The $MRT_{0-\infty}$ was determined as a ratio of $AUMC_{0-\infty}$ to $AUC_{0-\infty}$.

For allometric scaling, mean concentration versus time data from mice, rats, dogs, and rabbits (unpublished in house data) following E6201 IV administration was simultaneously modeled using a two-compartment body model with allometric scaling coefficients. Data were modeled using Scientist v. 2.0.1 (Micromath Inc, Salt Lake City, Utah, USA) as described by Gabrielsson and Weiner [4]. For predicting CL, allometric scaling with correction factor as suggested by the rule of exponent by Mahmood was applied [10]. The following allometric equation was applied.

$$Y = a \cdot W^b$$

where $Y$ is pharmacokinetic parameter of interest (clearance or volume), $W$ is the average weight of species in kg, and $a$ and $b$ are the coefficients and exponent of the allometric equation, respectively. The model-predicted parameters were used to predict human clearance and distribution volume and simulate the human pharmacokinetic profile at the proposed starting dose for Phase I clinical trial.

## Results

### In vitro studies

The mean plasma protein binding of E6201 ranged from 98.3 to 99.0% in mouse, 98.7 to 99.4% in rat, 98.0 to 98.7% in dog, and 98.2 to 98.4% in human plasma across 100–30000 ng/mL (Table 1).

The microsomal half-life as determined in NADPH-dependent E6201 depletion using a first-order decay equation in microsomal preparations was 84, 89, 70, and 36 min for mouse, rat, dog, and human, respectively.

No inhibition of major human CYPs (CYP1A2, 2C9, 2C19, 2D6, 2E1, and 3A) was detected in pooled human liver microsomes at 1–10 μM of E6201 (Table 2). The CYP-selective positive controls (data not shown) showed appropriate inhibitory effects for the respective probe reactions.

E6201 did not induce CYP3A, 2C9, or 2C19 at 1, 5, and 10 μM E6201 concentrations in human hepatocytes (Table 3). One donor (donor D at 10 μM E6201) showed slight CYP1A induction (~12.8% above vehicle), which was 3.7% of the induction observed with the positive control (20 nM TCDD). The results from Western blots (data not shown) also showed no detectable increase in CYP1A, 3A, 2C9, and 2C19 protein levels for any of the donors used in the induction assay.

### Pharmacokinetics in mice, rats, and dogs

Following IV administration in mice (Fig. 2), E6201 exhibited high plasma clearance (mean CL ranged from 5.68 to 7.46 L/h/kg, Table 4). The $V_{ss}$ was high and ranged from 3.12 to 4.83 L/kg. The mean elimination half-life ($t_{1/2}$) ranged from 0.4 to 1.0 h, indicating fast elimination of E6201 in mice. A nearly dose proportional increase in exposure with respect to dose of E6201 was observed in mice (Table 4). At 1 mg/kg dose, low levels of ER-813010 could be observed. Detectable levels of ER-813010 appeared in mouse plasma from 0.25 to 1 h and could be measured up to 4 or 6 h postdose of E6201. The mean elimination half-life ($t_{1/2}$) of ER-813010 ranged from 0.9 to 1.4 h in mice (Table 5). The metabolite to parent exposure ratio ($AUC_R$) was <4% in mice across the three doses.

In rats, following IV administration (Fig. 3), the systemic plasma CL of E6201 was high (mean CL ranged from 4.67 to 10.92 L/h/kg, Table 4), and the $V_{ss}$ was high (mean $V_{ss}$ ranged from 3.66 to 13.09 L/kg, Table 4). The mean $t_{1/2}$ ranged from 0.8 to 1.3 h. The exposure to E6201 in rats increased proportionally from 1 to 5 mg/kg, but more than proportionally from 5 to 10 mg/kg. In rats, measurable levels of ER-813010 appeared in plasma at 0.25 h and could be measured up to 8 h (4 h at 1 mg/kg dose) postdose of E6201. The mean elimination half-life ($t_{1/2}$) of ER-813010 ranged from 1.2 to 2.2 h in rats (Table 5). The $AUC_R$ was >20% in rats.

Following IV administration of E6201 in dogs (Fig. 4), the systemic plasma CL of E6201 was high (mean CL ranged from 2.11 to 3.45 L/h/kg, Table 4). The $V_{ss}$ was moderate (mean $V_{ss}$ ranged from 0.63 to 1.12 L/kg). The mean $t_{1/2}$ ranged from 0.6 to 1.6 h, suggesting fast elimination. The exposure to E6201 in dogs increased proportionally from 0.5 to 1.5 mg/kg, but less than proportionally from 1.5 to 5.0 mg/kg, (Table 5). Measurable levels of ER-813010 appeared in dog plasma at 0.25 h and could be monitored up to 12 h (4 h at 0.5 mg/kg dose) postdose of E6201. The mean elimination half-life ($t_{1/2}$) of ER-813010 ranged from 0.9 to 2.9 h in dogs across doses (Table 5). The $AUC_R$ was >29% in dogs.

### Allometric scaling and prediction of human pharmacokinetics

Human pharmacokinetics of E6201 was predicted using allometric scaling approach [4, 10]. A two-compartmental model with parameterization in terms of clearance (CL, Q) and volume of distribution ($V_1$, $V_2$) best described E6201 pharmacokinetics in all preclinical species. The allometry predicted an average plasma CL of 3.44 L/h/kg, an intercompartmental CL (Q) of 0.11 L/h/kg, a volume of distribution in the central compartment ($V_1$) of 7.29 L/kg, and a volume of distribution in the peripheral compartment ($V_2$)

**Table 1** Plasma protein binding of E6201

| Concentration of E6201 (ng/mL) | % protein binding (mean ± SD; $n = 3$) | | | |
|---|---|---|---|---|
| | Mouse | Rat | Dog | Human |
| 100 | 98.3 ± 0.1 | 98.7 ± 0.2 | 98.0 ± 0.1 | 98.3 ± 0.3 |
| 500 | 98.7 ± 0.3 | 98.9 ± 0.2 | 98.0 ± 0.3 | 98.3 ± 0.2 |
| 1,000 | 98.8 ± 0.4 | 99.4 ± 0.1 | 98.0 ± 1.2 | 98.4 ± 0.2 |
| 3,000 | 98.9 ± 0.3 | 99.2 ± 0.1 | 98.7 ± 3.3 | 98.4 ± 0.2 |
| 10,000 | 98.7 ± 0.3 | 99.2 ± 0.1 | 98.4 ± 0.4 | 98.2 ± 0.2 |
| 30,000 | 99.0 ± 0.2 | 99.1 ± 0.1 | 98.6 ± 0.2 | NT |

*SD* standard deviation, *NT* not tested

**Table 2** Evaluation of human CYP inhibition potential by E6201

| CYP450 | Metabolite formation rate (pmol/min/well)[a] | | | |
|---|---|---|---|---|
| | Vehicle | E6201 concentration (μM) | | |
| | | 1 | 5 | 10 |
| CYP1A2[b] | 5.7 ± 1.3 | 5.9 ± 1.3 | 4.6 ± 0.3 | 4.5 ± 0.8 |
| CYP2C19[c] | 38.4 ± 0.8 | 40.8 ± 2.7 | 37.9 ± 1.1 | 38.2 ± 2.2 |
| CYP2C9[d] | 8.3 ± 1.9 | 9.3 ± 0.1 | 8.1 ± 2.0 | 6.5 ± 0.4 |
| CYP2D6[e] | 14.3 ± 0.5 | 14.3 ± 1.0 | 13.6 ± 0.2 | 13.2 ± 0.5 |
| CYP2E1[f] | 456.9 ± 18.4 | 446.5 ± 13.7 | 452.5 ± 13.7 | 448.2 ± 19.9 |
| CYP3A[g] | 78.9 ± 4.0 | 82.1 ± 1.7 | 85.6 ± 4.0 | 84.6 ± 3.1 |
| CYP3A[h] | 456.3 ± 31.7 | 470.9 ± 15.0 | 509.0 ± 39.5 | 519.1 ± 29.7 |

Positive controls for respective CYP450 enzymes

[a] Mean ± SD ($n = 3$)

[b] R-warfarin 6-hydroxylation

[c] S-mephenytoin 4′-hydroxylation

[d] S-warfarin 7-hydroxylation

[e] bufuralol 1′-hydroxylation

[f] chlorzoxazone 6-hydroxylation

[g] midazolam 1′-hydroxylation

[h] midazolam 4-hydroxylation

**Table 3** Evaluation of human CYP induction potential by E6201

| Donor | Metabolite formation rate (pmol/min/well)[a] | | | | | |
|---|---|---|---|---|---|---|
| | Midazolam 1′-hydroxylation (CYP3A4/5) | | | Phenacetin *O*-deethylation (CYP1A) | | |
| | A | B | C | D | E | F |
| *Treatment* | | | | | | |
| Vehicle, MeOH | 1.33 ± 0.07 | 1.45 ± 0.13 | 9.46 ± 0.73 | 79.7 ± 3.32 | 2.91 ± 0.29 | 14.6 ± 1.31 |
| TCDD (20 nM) | NA | NA | NA | 429 ± 5.00 | 11.1 ± 0.98 | 337 ± 62.6 |
| RIF (50 μM) | 21.7 ± 0.75 | 2.50 ± 0.10 | 47.1 ± 2.16 | 93.6 ± 2.98 | 6.69 ± 0.68 | 4.00 ± 2.22 |
| E6201 (1 μM) | 1.59 ± 0.04 | <1.00[b] | 7.86 ± 0.08 | 84.0 ± 1.86 | <2.00[b] | 6.42 ± 0.16 |
| E6201 (5 μM) | 2.31 ± 0.20 | <1.00[b] | 5.40 ± 0.13 | 87.3 ± 1.88 | <2.00[b] | 12.2 ± 0.90 |
| E6201 (10 μM) | 2.40 ± 0.09 | <1.00[b] | 7.03 ± 0.29 | 92.5 ± 2.62 | 2.14 ± 0.15 | 10.3 ± 0.79 |
| Donor | Tolbutamide 4-methylhydroxylation (CYP2C9) | | | *S*-Mephenytoin 4′-hydroxylation (CYP2C19) | | |
| | G | H | I | J | K | L |
| *Treatment* | | | | | | |
| Vehicle, MeOH | 6.15 ± 0.43 | 7.71 ± 1.31 | 22.3 ± 0.91 | 5.92 ± 0.06 | 6.96 ± 0.29 | <0.50[b] |
| RIF (50 μM) | 28.2 ± 0.84 | 26.1 ± 5.86 | 46.3 ± 1.60 | 24.5 ± 2.15 | 20.1 ± 0.68 | 1.77 ± 0.16 |
| E6201 (1 μM) | 6.75 ± 1.43 | 7.78 ± 3.10 | 23.7 ± 1.04 | 6.49 ± 0.35 | 10.6 ± 1.68 | <0.50[b] |
| E6201 (5 μM) | 7.46 ± 1.13 | 8.43 ± 1.12 | 26.3 ± 2.22 | 7.20 ± 0.27 | 11.1 ± 1.26 | 0.78 ± 0.06 |
| E6201 (10 μM) | 9.24 ± 0.80 | 11.1 ± 0.68 | 27.3 ± 1.46 | 8.29 ± 0.14 | 11.7 ± 0.79 | <0.50[b] |

*MeOH* methanol, *TCDD* 2,3,7,8-tetrachlorodibenzo-*p*-dioxin, *RIF* rifampicin, *NA* not applicable

[a] Mean ± standard deviation ($n = 3$)

[b] Below quantification limit. Lower limit is given as the maximum value

of 3.29 L/kg in humans. Allometric scaling–based simulation and the observed human pharmacokinetic profile from the first-in-man trial are shown in Fig. 5. The allometry-predicted CL was 1.9-fold higher than the observed CL in first human subject, while the $V_1$ was overpredicted by approximately 70-fold.

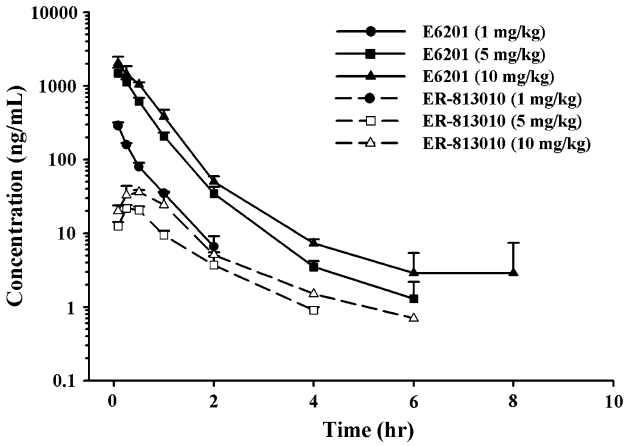


**Fig. 2** Plasma concentration versus time (mean ± SD, $n = 3$) profiles of E6201 (*solid line*) and ER-813010 (*broken line*) following 1, 5, and 10 mg/kg IV administration of E6201 in mice

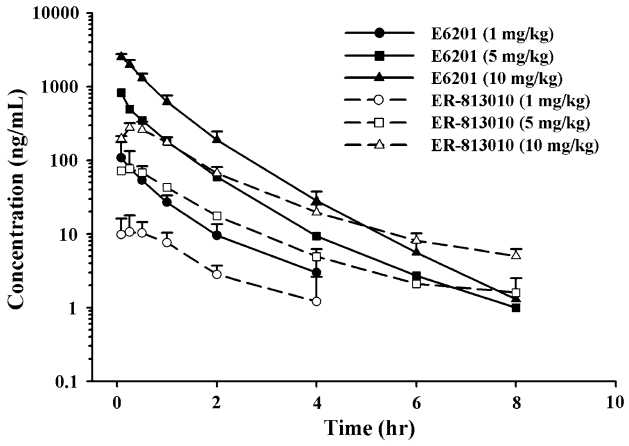


**Fig. 3** Plasma concentration versus time (mean ± SD, $n = 3$) profiles of E6201 (*solid line*) and ER-813010 (*broken line*) following 1, 5, and 10 mg/kg IV administration of E6201 in rats

**Table 4** Pharmacokinetic parameters of E6201 in mice, rats, and dogs following IV administration of E6201 ($n = 3$; $n = 4$ for dog)

| Species | Dose (mg/kg) | $AUC_{0-\infty}$ (ng h/mL) | $AUC_{0-\infty}$/D (ng h/mL/D) | CL (L/h/kg) | $V_{ss}$ (L/kg) | $t_{1/2}$ (h) |
|---|---|---|---|---|---|---|
| Mice | 1 | 140.3 | 140.3 | 7.13 | 3.54 | 0.4 |
| | 5 | 879.7 | 175.9 | 5.68 | 3.12 | 0.6 |
| | 10 | 1,341.2 | 134.1 | 7.46 | 4.83 | 1.0 |
| Rats[a] | 1 | 97.3 ± 31.3 | 97.3 ± 31.3 | 10.92 ± 2.97 | 13.09 ± 11.05 | 0.9 ± 0.5 |
| | 5[b] | 598.7 ± NC | 119.7 ± NC | 8.41 ± NC | 7.73 ± NC | 1.3 ± NC |
| | 10 | 2,161.6 ± 249.2 | 216.2 ± 24.9 | 4.67 ± 0.52 | 3.66 ± 0.18 | 0.8 ± 0.2 |
| Dogs[a] | 0.5 | 246.6 ± 52.4 | 493.2 ± 104.9 | 2.11 ± 0.50 | 0.63 ± 0.37 | 0.6 ± 0.1 |
| | 1.5 | 629.0 ± 221.2 | 419.3 ± 147.4 | 2.62 ± 0.91 | 0.87 ± 0.41 | 1.1 ± 0.2 |
| | 5 | 1,489.7 ± 301.1 | 297.9 ± 60.2 | 3.45 ± 0.65 | 1.12 ± 0.36 | 1.6 ± 1.3 |

*NC* not calculated

[a] Mean ± standard deviation

[b] $n = 2$

**Table 5** Pharmacokinetic parameters of ER-813010 in mice, rats, and dogs following IV administration of E6201 ($n = 3$; $n = 4$ for dog)

| Species | Dose[a] | $C_{max}$ (ng/mL) | $t^{b}_{max}$ (h) | $AUC_{0-\infty}$ (ng h/mL) | $t_{1/2}$ (h) | $AUC^{c}_{R}$ (%) |
|---|---|---|---|---|---|---|
| Mice | 1 | 1.6 | 1.0 | NC | NC | NC |
| | 5 | 21.7 | 0.25 | 27.0 | 0.9 | 3.1 |
| | 10 | 36.1 | 0.50 | 50.2 | 1.4 | 3.7 |
| Rats[d] | 1 | 11.7 ± 5.4 | 0.25 | 19.8 ± 0.63 | 1.2 ± 0.8 | 20.3 |
| | 5[e] | 76.6 ± NC | 0.25 | 123.8 ± NC | 2.2 ± NC | 20.7 |
| | 10 | 282.5 ± 52.1 | 0.25 | 462.4 ± 94.8 | 1.8 ± 0.3 | 21.4 |
| Dogs[d] | 0.5 | 75.0 ± 24.5 | 0.25 | 71.8 ± 17.9 | 0.9 ± 0.1 | 29.1 |
| | 1.5 | 239.1 ± 82.1 | 0.25 | 210.2 ± 59.4 | 2.9 ± 1.0 | 33.4 |
| | 5 | 519.0 ± 81.1 | 0.25 | 467.2 ± 73.9 | 2.9 ± 0.2 | 31.4 |

*NC* not calculated

[a] Dose of E6201 in mg/kg

[b] Median value (except for mouse)

[c] AUC ratio calculated as $(AUC_{0-\infty,\ ER\text{-}813010}/AUC_{0-\infty,\ E6201}) \times 100$

[d] Mean ± standard deviation

[e] $n = 2$

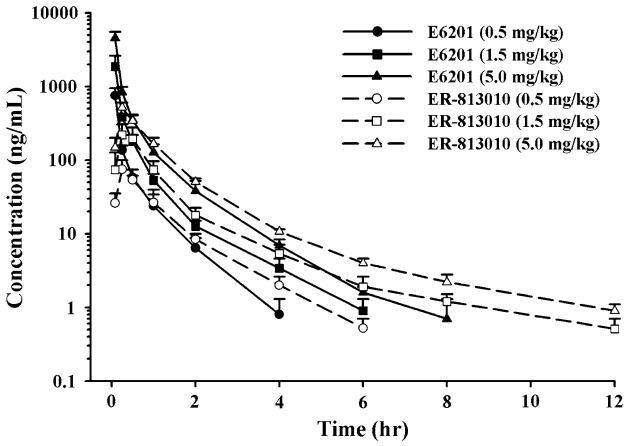


**Fig. 4** Plasma concentration versus time (mean ± SD, $n = 4$) profiles of E6201 (*solid line*) and ER-813010 (*broken line*) following 0.5, 1.5, and 5 mg/kg IV administration of E6201 in dogs

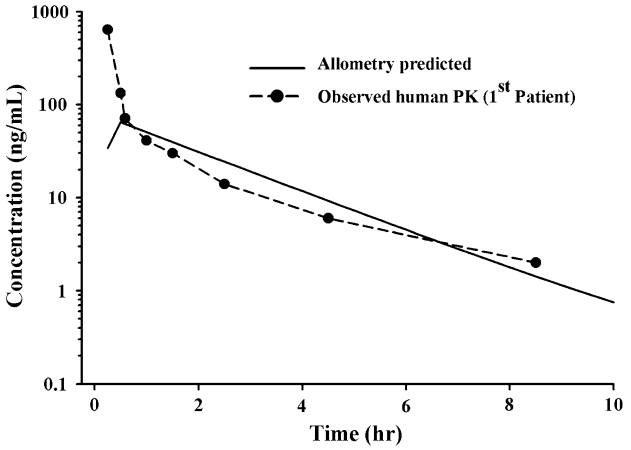


**Fig. 5** Observed (*filled circle*) and simulated (*solid line*) plasma concentration versus time profile of E6201 following a 30-min IV infusion of E6201 (20 mg/m$^2$) in humans

## Discussion

In the present work, the in vitro metabolism and pharmacokinetic characteristics of E6201, an anti-inflammatory and antihyperproliferative agent, were evaluated in preclinical species, and allometric scaling was applied to predict human pharmacokinetics.

The protein binding of E6201 (100–30,000 ng/mL) in mouse, rat, dog, and human plasma was high (>97%). In humans, mean plasma protein binding of E6201 ranged from 98.2 to 98.4% across the tested concentrations. Protein binding of E6201 was independent of the concentration and in general similar across the tested species. The in vitro metabolic stability studies of E6201 using microsomes exhibited species difference with human showing faster metabolic CL (microsomal half-life of 36 min) and rat with the highest metabolic stability (microsomal half-life of 89 min). However, there was a rapid conversion of E6201 to ER-813010 across all species tested in S9 fraction (unpublished in house data), suggesting that enzymes other than CYPs may be involved in E6201 metabolism. This may help explain the observed high plasma CL of E6201 in preclinical species.

Evaluation of CYP inhibition potential of E6201 using human microsomes resulted in no significant effects of E6201 on CYP isoform-selective activities. Thus, based on these data, E6201 is expected to have low potential for drug–drug interaction (DDI) in patients. Furthermore, no significant CYP induction was observed as determined using human hepatocytes. The minor CYP1A induction detected in one donor (donor D) did not approach the FDA's suggested threshold of 40% of the induction of the positive control and was only 12.8% greater than the vehicle [7]. In addition, the induction was only seen at the highest concentration of 10 μM. Therefore, based on the available data, the likelihood of DDI in patients due to E6201 CYP-mediated induction is anticipated to be low [1, 7].

The in vivo pharmacokinetics of E6201 in mice, rats, and dogs suggested high plasma CL of E6201 following IV administration. The distribution volume of E6201 was large in mice and rats, suggesting that E6201 distributes into extravascular tissues while in dogs the distribution was moderate. E6201 was rapidly eliminated with $t_{1/2}$ of <2 h in preclinical species.

The in vitro evaluation in a variety of human cancer cell line panel indicated that BRAF-mutated cell lines were sensitive to E6201 [11]. In mouse xenograft models, E6201 i.v administration (Q4D × 3 dosing regimen) resulted in a dose-dependent tumor growth delay or regression in three BRAF-mutated human cancer cell xenograft models and also demonstrated survival benefit in metastatic brain tumor model of BRAF-mutated MDA-MB-231 breast cancer cells [18]. Additionally, E6201 demonstrated a time-dependent inhibition of MEK 1 as measured by phospho-pRb in LOX tumors and decreased plasma IL-8 levels in V600E BRAF-mutated human melanoma-bearing mice at a single 40 mg/kg IV injection [18].

In the preclinical species, ER-813010, the isomeric metabolite of E6201, was observed across species as early as 0.25 h postdose, suggesting rapid in vivo conversion of E6201 to ER-813010. ER-813010 exhibited fast elimination ($t_{1/2}$ ranging from 0.9 to 2.9 h) similar to that of E6201 in all species. The $AUC_R$ ratio of ER-813010 was >10% in all species except mice at the studied dose levels of E6201.

For humans, the pharmacokinetic parameters of E6201 were predicted using allometric scaling, and the prediction suggested high CL and large volume of distribution as observed in preclinical species. A comparison of first human subject pharmacokinetics from Phase I indicated

that allometry yielded a good prediction of human CL although the distribution volume was overpredicted several folds (Fig. 5).

Overall, the pharmacokinetics of E6201 in preclinical species was described by high CL with large to moderate distribution. E6201 showed high protein binding independent of concentration across species. No significant CYP inhibition and CYP induction were observed in vitro, suggesting low risk of DDIs with E6201 in humans. In the first-in-human study, E6201 exhibited high CL, which was well predicted by allometric scaling.

**Acknowledgments** We would like to thank George Lai, Jesse (Jan-Shiang) Taur, Kenichi Nomoto, and Yuan Wang for their review and suggestions. We greatly acknowledge life sciences colleagues for conducting the in vivo animal studies.

**Conflict of interest** All authors (except Vipul Kumar and Zhi-Yi Zhang) are current employee of Eisai Inc. Vipul Kumar and Zhi-Yi Zhang were employee of Eisai Inc. at the time when some of this work was done.

## References

1. Bjornsson TD, Callaghan JT, Einolf HJ, Fischer V, Gan L, Grimm S, Kao J, King SP, Miwa G, Ni L, Kumar G, McLeod J, Obach RS, Roberts S, Roe A, Shah A, Snikeris F, Sullivan JT, Tweedie D, Vega JM, Walsh J, Wrighton SA (2003) The conduct of in vitro and in vivo drug–drug interaction studies: a Pharmaceutical Research and Manufacturers of America (PhRMA) perspective. Drug Metab Dispos 31(7):815–832
2. Davies H, Bignell GR, Cox C, Stephens P, Edkins S, Clegg S, Teague J, Woffendin H, Garnett MJ, Bottomley W, Davis N, Dicks E, Ewing R, Floyd Y, Gray K, Hall S, Hawes R, Hughes J, Kosmidou V, Menzies A, Mould C, Parker A, Stevens C, Watt S, Hooper S, Wilson R, Jayatilake H, Gusterson BA, Cooper C, Shipley J, Hargrave D, Pritchard-Jones K, Maitland N, Chenevix-Trench G, Riggins GJ, Bigner DD, Palmieri G, Cossu A, Flanagan A, Nicholson A, Ho JW, Leung SY, Yuen ST, Weber BL, Seigler HF, Darrow TL, Paterson H, Marais R, Marshall CJ, Wooster R, Stratton MR, Futreal PA (2002) Mutations of the BRAF gene in human cancer. Nature. ;417(6892):949–954
3. Ellestad GA, Lovell FM, Perkinson NA, Hargreaves RT, McGahren WJ (1978) New zearalenone related macrolides and isocoumarins from an unidentified fungus. J Org Chem 43:2339–2343
4. Gabrielsson J, Weiner D (2000) Pharmacokinetic and pharmacodynamic data analysis. Swedish pharmaceutical press, Stockholm, Sweden
5. Goto M, Chow J, Muramoto K, Chiba K, Yamamoto S, Fujita M, Obaishi H, Tai K, Mizui Y, Tanaka I, Young D, Yang H, Wang YJ, Shirota H, Gusovsky F (2009) E6201 [(3S, 4R, 5Z, 8S, 9S, 11E)-14-(ethylamino)-8, 9, 16-trihydroxy-3, 4-dimethyl-3, 4, 9, 19-tetrahydro-1H–2-benzoxacyclotetradecine-1, 7(8H)-dione], a novel kinase inhibitor of mitogen-activated protein kinase/extracellular signal-regulated kinase kinase (MEK)-1 and MEK kinase-1: In vitro characterization of its anti-inflammatory and antihyperproliferative activities. J Pharmacol Exp Ther 331(2): 485–495
6. Gregg CR (1999) Drug interactions and anti-infective therapies. Am J Med 106:227–237
7. Guidance for industry draft guidance (2006) Drug interaction studies—study design, data analysis, and implications for dosing and labeling. Available via DIALOG. http://www.fda.gov/downloads/Drugs/GuidanceComplianceRegulatoryInformation/Guidances/ucm072101.pdf. Accessed March 24, 2010
8. Lin JH, Lu AY (1997) Role of pharmacokinetics and metabolism in drug discovery and development. Pharmacol Rev 49(4):403–449
9. Lin JH, Lu AY (1998) Inhibition and induction of cytochrome P450 and the clinical implications. Clin Pharmacokinet 35:361–390
10. Mahmood I (2005) Interspecies pharmacokinetic scaling allometric principles and applications. Pine house publishers, Rockville, Maryland
11. Nomoto K, Wang J, Wu J, Agoulnik S, Kuznetsov G, Towle MJ, Schnaderbeck M, Gusovsky F, Shirota H, Littlefield BA (2009) In vitro antiproliferative activity of natural product-based MEK1 inhibitor E6201 against V600E BRAF-mutated cancer cell lines (abstract 3690). In: Annual meeting of the American Association for Cancer Research, Denver, CO. (18–22 April 2009)
12. Raucy JL, Mueller L, Duan K, Allen SW, Strom S, Lasker JM (2002) Expression and induction of CYP2C P450 enzymes in primary cultures of human hepatocytes. J Pharmacol Exp Ther 302:475–482
13. Runge D, Kohler C, Kostrubsky VE, Jager D, Lehmann T, Runge DM, May U, Stolz DB, Strom SC, Fleig WE, Michalopoulos GK (2000) Induction of cytochrome P450 (CYP)1A1, CYP1A2, and CYP3A4 but not of CYP2C9, CYP2C19, multi-drug resistance (MDR-1) and multi-drug resistance associated protein (MRP-1) by prototypical inducers in human hepatocytes. Biochem Biophys Res Commun 273:333–341
14. ShenY BoivinR, Yoneda N, Du H, Schiller S, Matsushima T, Goto M, Shirota H, Gusovsky F, Lemelin C, Jiang Y, Zhang Z, Pelletier R, Ikemori-Kawada M, Kawakami Y, Inoue A, Schnaderbeck M, Wang Y (2010) Discovery of anti-inflammatory clinical candidate E6201, inspired from resorcylic lactone LL-Z1640–2, III. Bioorganic Medicinal chemistry letter 20: 3155–3157
15. Wallace EM, Lyssikatos JP, Yeh T, Winkler JD, Koch K (2005) Progress towards therapeutic small molecule MEK inhibitors for use in cancer therapy. Curr Top Med Chem 5(2):215–229
16. Wang JY, Wilcoxen KM, Nomoto K, Wu S (2007) Recent advances of MEK inhibitors and their clinical progress. Curr Top Med Chem 7(14):1364–1378
17. Whitlock JP Jr (1999) Induction of cytochrome P4501A1. Annu Rev Pharmacol Toxicol 39:103–125
18. Wu J, Nomoto K, Wang J, Kuznetsov G, Agoulnik S, Shuck E, Wong N, Towle MJ, Schnaderbeck M, Wu S, Littlefield BA (2009) In vivo anticancer activity of E6201, a novel MEK1 inhibitor, against BRAF-mutated human cancer xenografts (abstract 3687). In: Annual meeting of the American Association for Cancer Research, Denver, CO. (18–22 April 2009)
19. Xu L, Li AP, Kaminski DL, Ruh MF (2000) 2, 3, 7, 8 Tetrachlorodibenzo-p- dioxin induction of cytochrome P4501A in cultured rat and human hepatocytes. Chem Biol Interact 124:173–189

Journal of Biomolecular Screening
18(2) 199–210

DOI: 10.1177/1087057112463732
http://jbx.sagepub.com
SAGE

# Application of a Substrate Cocktail Approach in the Assessment of Cytochrome P450 Induction Using Cultured Human Hepatocytes

**Robert D. Pelletier[1,2], W. George Lai[1], and Y. Nancy Wong[1]**

**Abstract**

Induction of the cytochrome P450 (CYP) family of enzymes by coadministered compounds can result in drug-drug interactions, as in the case of the coadministration of rifampicin with many CYP3A substrates, including midazolam. Identification of potential drug-drug interactions due to CYP induction during drug discovery is critical. We present a substrate cocktail method that was applied to assess the induction of CYP1A, CYP2B6, CYP2C9, and CYP3A using a 96-well high-throughput format. Viable cell counts were determined using a high-content screening system to normalize activities. Substrate cocktail incubations demonstrated a similar fold induction for known inducers as compared with discrete probe incubations. The system was further validated by determining the induction potency of rifampicin. The $E_{max}$ and $EC_{50}$ values in two separate lots of hepatocytes for CYP3A induction by rifampicin in a 96-well format were similar when discrete probe was compared with the probe cocktail. This system has been demonstrated to be suitable for high-throughput assessments of CYP induction.

**Keywords**

CYP induction, high-throughput screening, drug-drug interaction

## Introduction

The importance of the CYP family of enzymes in drug disposition and safety is well documented. The CYP family of enzymes is estimated to be responsible for greater than 75% of the known metabolism of therapeutic agents, and alteration of CYP activity can have a significant influence on the disposition of pharmaceutical agents used today, resulting in undesirable effects.[1]

CYP activities can be altered by inducing the expression of a CYP and its reaction cycle partners, including P450 reductase.[2,3] This increase in expression may result in an increase of CYP activity, which can lead to increasing metabolite(s) levels and could be potentially toxic. Many clinically relevant examples of the CYP induction phenomena exist such as the induction of CYP1A by tobacco smoke inhalation and CYP3A by carbamazepine and rifampicin.[4,5]

CYP induction is usually the result of signaling through nuclear receptors that are capable of binding to the xenobiotic response elements (XREs) located in the gene locus of the respective CYP.[2,6] Four of the important nuclear receptors are the aryl hydrocarbon receptor (AhR), pregnane X receptor (PXR), retinoid X receptor (RXR), and constitutive androstane receptor (CAR).[2,7] PXR, RXR, and CAR usually function as heterodimer partners with other nuclear receptors by binding of a ligand and then binding to XREs in the gene locus of an inducible CYP. Cytochromes P450 2B6, 2C9, 3A4, and 3A5 all contain XREs for these three receptors and, therefore, can be induced through their signaling.[2,6] There is some purported preference for these receptors due to gene locus content of the respective XREs, such as CAR with CYP2B6 and PXR with CYP3A, but the individual responses may vary significantly.[8]

The potential induction of CYPs can be assessed in multiple ways, including activity, mRNA analysis such as quantitative polymerase chain reaction (qPCR), and protein

[1]Eisai, Inc., Andover, MA, USA
[2]Current address: Department of Medicinal Chemistry, University of Washington, Seattle, WA, USA

Received May 31, 2012, and in revised form Jul 19, 2012. Accepted for publication Sep 12, 2012.

**Corresponding Author:**
Robert D. Pelletier, Department of Medicinal Chemistry, University of Washington, Seattle, WA, USA
Email: rbrtpelletier@gmail.com

analysis such as enzyme-linked immunosorbent assay (ELISA) or Western blotting.[9] The measurement of mRNA allows for several forms to be analyzed simultaneously, but the increase in mRNA does not proportionally increase the functional CYP content. Factors, such as the translation efficiency of apo-protein from mRNA and posttranslational modifications, limit the direct correlation of increased mRNA content to increased CYP activity. However, it can serve to avoid potential false-negative results with regard to induction signal transduction experienced by other approaches.[10] Protein analysis is limited by the availability of highly selective antibodies for closely related CYP forms. Direct correlation to activity could also be hindered by factors such as heme incorporation and compound inhibition or inactivation.[11] Since it demonstrates the end result of the change in CYP activity, activity measurement is usually more desirable. Members of the CYP enzyme family tend to have overlapping substrate specificities, but selective probes, which are critical for accurate measurement, are well described in the literature.[12]

In this study, we measured the activities of CYP forms using probes individually or as a cocktail in 24-well plated and 96-well plated hepatocytes to show the feasibility of a substrate cocktail approach in the analysis of CYP1A, CYP2B6, CYP2C9, and CYP3A. This approach has been used in other studies as well.[13–15] However, we also coupled the assessment of the viable cell count using a Cellomics (Pittsburgh, PA) instrument for normalization of enzyme activity and detection of possible cytotoxicity, and we investigated induction of unintended CYP forms by prototypical inducers to ensure the results were not an artifact of the cocktail probe system.

## Materials and Methods

### Materials

$^{13}C_2$-,$^{15}$N-Acetaminophen, $^{2}H_6$-hydroxybupropion, $^{2}H_9$-hydroxytolbutamide, $^{13}C_3$-1′-hydroxymidazolam, plateable cryopreserved human hepatocytes, and 24-well collagen I–coated plates were purchased from BD Biosciences (Woburn, MA). Black-walled, clear-bottom, collagen I–coated 96-well plates were purchased from Thermo Scientific (Rochester, NY). Cryopreserved hepatocyte recovery media (CHRM), 4′,6-diamidino-2-phenylindole (DAPI), William's E media, and plating and maintenance media supplements were purchased from Invitrogen (Carlsbad, CA). Dulbecco's modified Eagle's media (DMEM), Dulbecco's phosphate buffered saline (DPBS), fetal bovine serum (FBS), penicillin/streptomycin/glutamine, and minimal essential medium (MEM) nonessential amino acids were purchased from Mediatech (Manassas, VA). Acetaminophen, carbamazepine, clozapine, coumestrol, (±)-ibuprofen, ketoconazole, lovastatin, metoprolol, β-naphthoflavone, phenacetin, phenobarbital, phenytoin, rifampicin, and tolbutamide were purchased from Sigma Aldrich (St. Louis, MO). Bupropion, dextromethorphan, dextrorphan, $^{2}H_3$-dextrorphan, hydroxybupropion, hydroxytolbutamide, 1′-hydroxymidazolam, and midazolam were purchased from Toronto Research Chemical (Toronto, Canada). Nevirapine, ritonavir, DL-sulforaphane, and troglitazone were also purchased from commercial sources. All chemicals, reagents, and solvents used in this study were of either analytical or high-performance liquid chromatography (HPLC) grade.

### Plating and Treatment of Hepatocytes

Cryopreserved hepatocytes were plated after isolation using CHRM at 375 000 cells/well for 24-well plates or 60 000 cells/well for 96-well plates. For 96-well plates, 50 µL/well of DMEM containing 10% FBS, 1 U/mL penicillin, 1 µg/mL streptomycin, 0.292 mg/mL L-glutamine, and nonessential amino acids was added before 80 µL of plating media from Invitrogen (part # CM3000 and A1217601) containing 0.75 million cells/mL was gently added to the well. Hepatocytes were allowed to attach overnight in an incubator at 37 °C and 5% $CO_2$.

Cells were treated with 500 µL (24-well) or 100 µL (96-well) of maintenance media (Invitrogen, part # CM4000 and A1217601) containing vehicle (0.1% DMSO), β-naphthoflavone (10 µM), phenobarbital (1 mM), or rifampicin (0.32–25 µM). The maintenance medium was refreshed daily during the 48-h treatment.

### CYP Activity Assay

After treatment, the maintenance media were replaced by the same volume of DPBS containing either a discrete probe substrate or a probe substrate cocktail. The probe substrates used were 100 µM phenacetin 200 µM bupropion, 200 µM tolbutamide, and 50 µM midazolam for assessments of CYP1A, CYP2B6, CYP2C9, and CYP3A activities, respectively. Midazolam was used at concentrations above $K_m$ to avoid depletion of the substrate that would result in possible underestimation of induction. The cells were incubated for 20 min prior to extracting a small amount of the incubation buffer for analysis. The cells were washed with DPBS after the incubation. An equal volume of a 1:1 acetonitrile/methanol solution containing 50 ng/mL of $^{13}C_2$-,$^{15}$N-acetaminophen, $^{2}H_6$-hydroxybupropion, $^{2}H_9$-hydroxytolbutamide, or $^{13}C_3$-1′-hydroxymidazolam was added to the incubated DPBS to provide an internal standard for each analyte.

To test the influence of PXR activation on CYP2D6 activity, 20 µM dextromethorphan was used as a probe substrate and incubated for 20 min with treated cells. An equal volume of a 1:1 acetonitrile/methanol solution containing

50 ng/mL of $^{2}H_{3}$-dextrorphan was added to the incubated DPBS to provide an internal standard.

The incubated samples were analyzed using a system consisting of an API 4000QTrap (AB Sciex, Foster City, CA) and an HPLC system consisting of two LC-10ADvp series HPLC pumps, a SIL-HTC autosampler, a CTO-10ACvp column oven, and a DGU-14A column oven (Shimadzu, Kyoto, Japan) or consisting of a TripleTOF 5600 (AB Sciex) and an ultra-performance liquid chromatography (UPLC) system consisting of two LC-30AD series UPLC pumps, a SIL-30AC autosampler, a CTO-30A column oven, and a DGU-20A5R column oven (Shimadzu). The column was a Sunfire $C_{18}$ 2.1 × 150–mm, 5-µ column from Waters Corporation (Milford, MA), and mobile phases were (a) 0.02% formic acid in water and (b) 0.02% formic acid in acetonitrile. The binary gradient was the following: 0% B (0–0.5 min), 0% to 99% B (0.5–4 min), 99% B (4–4.5 min), and 0% B (4.6–8 min). A standard curve containing 2 nM to 1 µM of each metabolite of interest was used to quantify the formation of acetaminophen, hydroxybupropion, hydroxytolbutamide, and 1′-hydroxymidazolam to assess the activities of CYP1A, CYP2B6, CYP2C9, and CYP3A, respectively.

### Assessment of Cell Viability

After washing with DPBS, the cells were fixed using 3.7% *p*-formaldehyde in DPBS for 1 h. The formaldehyde was removed and 0.6 µM DAPI in DPBS was added. The cells were stained by DAPI for 20 min and then washed three times with DPBS. Cells were counted using an ArrayScan II (Cellomics) with a 5× objective lens. This step was performed with only 96-well plates due to the limitations of the ArrayScan II instrument, and the results were used to normalize activities in 96-well plates to a per cell basis by the following equation:

$$\text{Activity} = \frac{[\text{Metabolite of CYP probe}] * 100\ \mu\text{L}}{20\ \text{min} * \text{cell number}}.$$

### Analysis of mRNA via Quantitative Real-Time PCR

Isolation of mRNA from 24-well plated human hepatocytes was performed using an RNeasy kit from Qiagen (Valencia, CA). Reverse transcription was performed using a SuperScript VILO cDNA Synthesis Kit from Invitrogen (Grand Island, NY) and a DNA Engine thermocycler from Bio-Rad (Hercules, CA). Nuclease-free water was acquired from Invitrogen (Grand Island, NY). Real-time PCR was performed using a 7500 Fast Real Time PCR System and TaqMan Fast Advanced Master Mix from Applied Biosystems (Carlsbad, CA). The assays were performed in duplex or triplex using β-2-microglobulin (B2M) as an endogenous control in the FAM channel and the genes of interest in the VIC channel and NED channel, and the data were assessed via $\Delta\Delta C_t$ calculations to determine fold induction. B2M was chosen from a panel of endogenous controls (Applied Biosystems human endogenous control plate, part # 4426700) due to its low variation between vehicle and positive control treatment groups after mRNA content normalization and due to the specificity of the probe and primer set. The following TaqMan probes and primer assay sets from Applied Biosystems were used for these assays in a primer-limited format: Hs00984230_m1 (B2M), Hs00167927_m1 (CYP1A2), Hs04183483_g1 (CYP2B6), HS04260376_m1 (CYP2C9), Hs02576168_g1 (CYP2D6), HS00604506_m1 (CYP3A4), Hs01016332_m1 (P450 oxidoreductase), Hs00609293_g1 (hydroxymethylbilane synthase), and Hs00167441_m1 (aminolevulinate, delta-, synthase 1). Student's *t* test was used to determine if a treatment caused any changes as compared with vehicle control.

## Results and Discussion

### Comparison of Results for Known Inducers with Discrete Probes or Substrate Cocktail

For the substrate cocktail to be suitable for the assessment of CYP induction, the fold induction response to an inducer should match the observed results with a discrete probe. As shown in **Tables 1** to **3**, the fold induction for known inducers using lots 246 and 262 are similar among discrete and substrate cocktail incubations. The 96-well activities were normalized by cell number as acquired from a Cellomics instrument, whereas no normalization was performed with 24-well results.

For CYP1A, the fold induction after treatment with β-naphthoflavone was not affected by the use of a substrate cocktail. The results from lot 246 (**Tables 1** and **2**) showed similar results in both 24- and 96-well formats, as well as discrete probes and substrate cocktails. The fold induction after treatment for this lot ranged from 18- to 27-fold. The basal level of activity and induced level of activity for CYP1A appeared to be reduced by 30% to 45% with the use of a substrate cocktail with lot 246. A possible explanation is competition between the CYP forms for limited amounts of P450 reductase.[16] The results obtained from lot 262 (**Table 3**) appeared to be less affected by the use of the substrate cocktail. The basal activity increased by 23% but was not significant, by Student's *t* test, due to the variation evidenced by the standard deviation. The induced activity was reduced by 15%, which was a smaller effect than that shown with lot 246. The CYP1A activity resulting from the use of a substrate cocktail did not alter the fold induction. The CYP1A results from the substrate cocktail suggest indirect induction effects by the known inducers for other CYP forms. Phenobarbital and rifampicin, which are not known to signal through the AhR pathway, increased CYP1A activity in both donors.[2,17]

**Table 1.** Fold Induction from a 24-well Format with Lot 246

| | Activity (pmol/min/well) | | | | Fold Induction | | | |
|---|---|---|---|---|---|---|---|---|
| Inducer | CYP1A | CYP2B6 | CYP2C9 | CYP3A | CYP1A | CYP2B6 | CYP2C9 | CYP3A |
| | | | | **Discrete probe** | | | | |
| Vehicle | 2.00 ± 0.19 | 1.43 ± 0.13 | 1.98 ± 0.16 | 1.05 ± 0.03 | — | — | — | — |
| β-NF 10 μM | 42.6 ± 2.4 | — | — | — | **21.3** | — | — | — |
| PB 1 mM | — | 3.79 ± 0.72 | — | — | — | **2.7** | — | — |
| Rif 10 μM | — | 18.0 ± 1.2 | 12.65 ± 1.08 | 39.2 ± 5.0 | — | 12.6 | **6.4** | **37.3** |
| | | | | **Substrate cocktail** | | | | |
| Vehicle | 1.09 ± 0.11 | 1.01 ± 0.04 | 2.22 ± 0.02 | 0.87 ± 0.07 | — | — | — | — |
| β-NF 10 μM | 29.7 ± 1.2 | 3.20 ± 0.12 | 3.47 ± 0.42 | 1.54 ± 0.20 | **27.3** | 3.2 | 1.6 | 1.8 |
| PB 1 mM | 1.66 ± 0.29 | 2.52 ± 0.57 | 1.83 ± 0.23 | 5.72 ± 1.31 | 1.5 | **2.5** | 0.8 | 6.6 |
| Rif 10 μM | 8.24 ± 1.06 | 11.2 ± 1.0 | 9.15 ± 0.79 | 35.2 ± 0.5 | 7.6 | 11.1 | **4.1** | **40.5** |

n = 3. Data are expressed as mean ± SD. —, not applicable (vehicle) or not tested (all others); β-NF, β-naphthoflavone; PB, phenobarbital; Rif, rifampicin. Bold values are from treatment by a typical inducer for that form.

**Table 2.** Fold Induction from a 96-well Format with Lot 246

| | Activity (pmol/min/$10^6$ cells) | | | | Fold Induction | | | |
|---|---|---|---|---|---|---|---|---|
| Inducer Inducer | CYP1A | CYP2B6 | CYP2C9 | CYP3A | CYP1A | CYP2B6 | CYP2C9 | CYP3A |
| | | | | **Discrete probe** | | | | |
| Vehicle | 13.4 ± 0.7 | 4.56 ± 2.00 | 10.5 ± 0.5 | 6.29 ± 1.05 | — | — | — | — |
| β-NF 10 μM | — | — | — | — | **20.7** | — | — | ND |
| PB 1 mM | — | 36.1 ± 6.7 | — | — | — | **7.9** | — | — |
| Rif 10 μM | — | 72.8 ± 11.9 | 37.0 ± 5.9 | 155 ± 17 | — | 16.0 | **3.5** | **24.6** |
| | | | | **Substrate cocktail** | | | | |
| Vehicle | 8.98 ± 1.50 | 2.23 ± 0.56 | 9.14 ± 1.95 | 4.11 ± 0.37 | — | — | — | — |
| β-NF 10 μM | 162 ± 15 | 8.14 ± 0.75 | 10.2 ± 0.2 | 4.65 ± 1.20 | **18.1** | 3.7 | 1.1 | 1.1 |
| PB 1 mM | 21.0 ± 2.3 | 25.8 ± 4.3 | 16.5 ± 1.2 | 72.8 ± 13.6 | 2.3 | **11.6** | 1.8 | 17.7 |
| Rif 10 μM | 39.4 ± 3.5 | 55.3 ± 9.2 | 26.9 ± 5.6 | 140 ± 3 | 4.4 | 24.8 | **2.9** | **34.2** |

n = 3. Data are expressed as mean ± SD. —, not applicable (vehicle) or not tested (all others); β-NF, β-naphthoflavone; PB, phenobarbital; Rif, rifampicin. Bold values are from treatment by a typical inducer for that form.

Rifampicin increased CYP1A activity up to 7.6-fold. The increase of activity was not as strong as with β-naphthoflavone but was substantial. Since CYP1A mRNA is not known to be increased by treatment with rifampicin, it is likely due to other processes. Induction of P450 oxidoreductase or other factors involved in the regulation of CYP activity by the PXR and CAR pathways may explain this phenomenon.[3,18] These data suggest a mechanism for disconnection between mRNA levels and enzyme activity for the induction of a CYP form.

For CYP2B6, the fold induction also did not appear to be affected by the use of a substrate cocktail. The reduction of measured basal and induced CYP2B6 activities using a substrate cocktail was consistent between the two donors and was consistent in affecting both the negative control and positive control to a similar extent. The basal and induced activities were affected equally, so fold induction was not affected. With these two donors, rifampicin at 10 μM showed equal or greater potency of CYP2B6 induction as compared with phenobarbital at 1 mM. There is a discrepancy between the 24-well and 96-well format for fold induction of CYP2B6 for lot 246, but the reason is unknown.

As seen with CYP1A, CYP2B6 activity was also increased by an inducer that was not known to affect the signaling pathway that regulates mRNA levels of CYP2B6. Treatment with β-naphthoflavone, an AhR ligand, increased CYP2B6 activity by approximately 3-fold in each condition tested. The reason for this increase is speculated to be similar to that for CYP1A.[2,3]

To investigate the observed phenomenon of increased phenacetin O-deethylase activity observed with rifampicin and increased bupropion hydroxylase activity observed with β-naphthoflavone, a comparison was done using incubations with phenacetin as a discrete probe, bupropion as a discrete probe, or the substrate cocktail using lot 246. The

**Table 3.** Fold Induction from a 96-well Format with Lot 262

| Inducer | Activity (pmol/min/$10^6$ cells) | | | | Fold Induction | | | |
|---|---|---|---|---|---|---|---|---|
| | CYP1A | CYP2B6 | CYP2C9 | CYP3A | CYP1A | CYP2B6 | CYP2C9 | CYP3A |
| | | | | **Discrete probe** | | | | |
| Vehicle | 13.9 ± 1.2 | 3.15 ± 0.23 | 5.35 ± 0.43 | 42.3 ± 3.3 | — | — | — | — |
| β-NF 10 μM | 425 ± 7 | — | — | — | **30.6** | — | — | — |
| PB 1 mM | — | 35.4 ± 6.2 | — | — | — | **11.2** | — | — |
| Rif 10 μM | — | 36.4 ± 2.5 | 22.3 ± 5.7 | 363 ± 22 | — | 11.6 | **4.2** | **8.6** |
| | | | | **Substrate cocktail** | | | | |
| Vehicle | 17.1 ± 2.6 | 1.44 ± 0.58 | 6.87 ± 1.37 | 46.0 ± 6.4 | — | — | — | — |
| β-NF 10 μM | 360 ± 7 | 4.94 ± 0.47 | 10.7 ± 2.1 | 36.0 ± 0.6 | **21.0** | 3.4 | 1.5 | 0.8 |
| PB 1 mM | 60.8 ± 5.2 | 18.7 ± 2.2 | 23.5 ± 5.5 | 320 ± 31 | 3.6 | **13.0** | 3.4 | 7.0 |
| Rif 10 μM | 87.6 ± 4.8 | 19.2 ± 2.3 | 28.9 ± 2.5 | 366 ± 41 | 5.1 | 13.3 | **4.2** | **8.0** |

n = 3. Data are expressed as mean ± SD. —, not applicable (vehicle) or not tested (all others); β-NF, β-naphthoflavone; PB, phenobarbital; Rif, rifampicin. Bold values are from treatment by a typical inducer for that form.

increase in activity was also observed in discrete probe incubations and, therefore, is not a unique phenomenon of the cocktail probe as shown by **Table 4**.

Three approaches were taken to elucidate the source of apparent induction by β-naphthoflavone and rifampicin. The first was using a CYP2D6 probe to see if the activity increased after cells were treated with rifampicin or β-naphthoflavone. The second was the use of qPCR analysis to analyze mRNA expression of CYP genes and genes of others proteins involved in CYP regulation. The third approach was the use of PXR inhibitors, such as coumestrol, ketoconazole, and DL-sulforaphane, to attempt to isolate the effect of rifampicin on CYP1A activity to the PXR signaling pathway.[19–21]

There was an increase in CYP2D6-mediated dextromethorphan O-demethylation activity after the treatment with rifampicin and β-naphthoflavone, to a much smaller extent, even though there was no induction of CYP2D6 mRNA (**Table 4**). CYP1A2 mRNA was not significantly increased with the rifampicin, but there was a small increase in CYP2B6 mRNA expression with β-naphthoflavone. Since mRNA levels for CYP1A2 did not correlate with the increased activity, it is possible that other genes involved in CYP regulation could be involved in the increase of CYP1A and CYP2D6 activity.

To investigate a possible explanation for the disconnection between activity and mRNA, mRNA analysis was performed for some genes that are involved in the CYP reaction cycle and in heme biosynthesis. The mRNA expression of aminolevulinate synthase 1 (ALAS1), a protein involved in heme biosynthesis, was increased by rifampicin and β-naphthoflavone, but mRNA of hydroxymethylbilane synthase, another protein involved in heme biosynthesis, was not affected.[22,23] Also, rifampicin weakly induced P450 oxidoreductase mRNA expression, but β-naphthoflavone did not. The induction of mRNA for other proteins involved in the reaction cycle of CYP or involved in the synthesis of heme, which can be incorporated into CYP, shows there is potential to increase CYP activity even if the mRNA of the particular CYP being measured is not being induced.

To study the potential effects of PXR inhibitors, cells were treated with 20 μM coumestrol, 25 μM ketoconazole, or 1 mM DL-sulforaphane, which are concentrations near their reported $IC_{50}$ values for PXR in the absence or presence of rifampicin.[19–21] Coumestrol had no effect on rifampicin induction of CYP3A activity at 20 μM, and a treatment of 100 μM coumestrol resulted in over 60% cell number reduction. The treatments for ketoconazole and DL-sulforaphane resulted in approximately 50% cell number reduction as compared with non-PXR-treated controls. There was a reduction in induction on a per cell basis for all cytotoxic concentrations of PXR inhibitors, but as suggested by the reduction in cell number, the effects of normal cellular function impairment cannot be separated from any potential PXR inhibition (data not shown).

The activity and mRNA data suggest two different scenarios for the effect of rifampicin on CYP1A activity and for the effect of β-naphthoflavone on CYP2B6 activity. Rifampicin appears to affect CYP1A activity via indirect mechanisms of induction, including possibly P450 oxidoreductase expression and heme incorporation. β-Naphthoflavone may have direct and indirect effects on CYP2B6 activity since CYP2B6 mRNA was increased but ALAS1 mRNA was also increased. These data also do not rule out the possibility of posttranscriptional regulation of CYP genes that could lead to increased efficiency of expression of CYP functional proteins that are generically regulated through PXR and AhR signaling pathways.

As expected, CYP2C9 induction was weaker than the other forms examined.[2] With lot 246, there was a small reduction of

**Table 4.** Effect of Rifampicin and β-naphthoflavone on CYP Activity and mRNA Levels of CYP Forms and Genes Involved in CYP Regulation

| | Rif 10 μM (Fold) | | β-NF 10 μM (Fold) |
|---|---|---|---|
| **Activity** | | | |
| Phenacetin O-deethylase with discrete probe | 4.1 ± 0.1 | Bupropion hydroxylase with discrete probe | 1.7 ± 0.3 |
| Phenacetin O-deethylase with substrate cocktail | 6.0 ± 0.6 | Bupropion hydroxylase with substrate cocktail | 1.7 ± 0.1 |
| Dextromethorphan O-demethylation with discrete probe | 3.1 ± 0.2 | Dextromethorphan O-demethylation with discrete probe | 1.8 ± 0.2 |
| **mRNA** | | | |
| CYP1A2 | 1.6 ± 0.1 | CYP1A2 | 125.1 ± 23.5 |
| CYP2B6 | 8.7 ± 0.6 | CYP2B6 | 3.6 ± 0.1 |
| CYP2C9 | 2.0 ± 0.1 | CYP2C9 | 0.8 ± 0.1 |
| CYP2D6 | 1.2 ± 0.2 | CYP2D6 | 0.7 ± 0.2 |
| CYP3A4 | 132.0 ± 9.1 | CYP3A4 | 0.3 ± 0.0 |
| P450 OR | 2.5 ± 0.1 | P450 OR | 1.3 ± 0.1 |
| HMBS | 1.2 ± 0.1 | HMBS | 1.5 ± 0.3 |
| ALAS1 | 5.4 ± 0.3 | ALAS1 | 3.0 ± 0.2 |

n = 3. Data are expressed as mean ± SD. Rif, rifampicin; β-NF, β-naphthoflavone; P450 OR, P450 oxidoreductase; HMBS, hydroxymethylbilane synthase; ALAS1, aminolevulinate, delta-, synthase 1.

activity using the substrate cocktail with the induced cells, and the vehicle was relatively unchanged. The use of the substrate cocktail did not appear to influence the measurement of CYP2C9 activity with lot 262. The fold induction was similar in the discrete and substrate cocktail with both donors.

CYP3A activity did not seem to be affected by the use of the substrate cocktail. With both hepatocyte lots and incubation formats, some differences in fold induction were observed between discrete and substrate cocktails. However, this was likely due to the variation in the vehicle control since the induced activity levels were very similar as measured by discrete or substrate cocktails.

As a further validation of the use of the substrate cocktails for induction assessment, $EC_{50}/E_{max}$ curves for CYP3A induction by rifampicin were generated and compared among the discrete and substrate cocktails. These curve fits were conducted via four-parameter fitting. As shown in **Figure 1**, the $EC_{50}$ values for a given lot were highly consistent, whereas there was more variation among $E_{max}$ values. Since the fold induction is measured against the vehicle control for CYP activity, variation in vehicle control activity would influence the $E_{max}$ values. **Figure 1D** shows the relationship of rifampicin concentration to activity with the discrete probe and substrate cocktail using data used to generate **Figure 1B**. The two curves are almost indistinguishable, with the greatest differences being the vehicle control. In **Figure 1C**, the higher $E_{max}$ value for rifampicin was seen with the discrete probe as opposed to the substrate cocktail; therefore, the use of the substrate cocktail may not be responsible for the differences in the estimated $E_{max}$ values. It appears that the substrate cocktail did not influence the estimation of the CYP3A induction potency by rifampicin.

## *Impact Analysis of Normalization by Cell Count on CYP Activity*

The use of cell counts allows the determination of concentration-dependent cell number reduction by potentially cytotoxic compounds such as the PXR inhibitors coumestrol, ketoconazole, and DL-sulforaphane. Without measuring the impact on cell number or cell viability by these compounds, the cause in reduction of CYP activity may not be properly assessed due to lack of information on cellular function. This potential situation could apply with inducers that are being used above the tolerated concentrations in hepatocytes, which would result in underestimation of potency or a false-negative result.

To assess the ability of cell counts to reduce analytical variation, the coefficient of variation (CV) was calculated with and without cell count normalization for lots 246 and 267 CYP activities, as shown in **Table 5**. The mean % CV is very similar with and without normalization, so the normalization does not appear to aid in reducing variation. The cell numbers were consistent, with a % CV of 6.7% for lot 246 and 12.7% for lot 262; therefore, the utility of normalization may be limited in terms of reducing variation in activity since the plating of cells appeared to be reproducible.

The positive impact of cell counts appears to be limited to the accuracy of assessing the data being generated. However, this aspect is essential in properly interpreting the results generated from the activity assay.

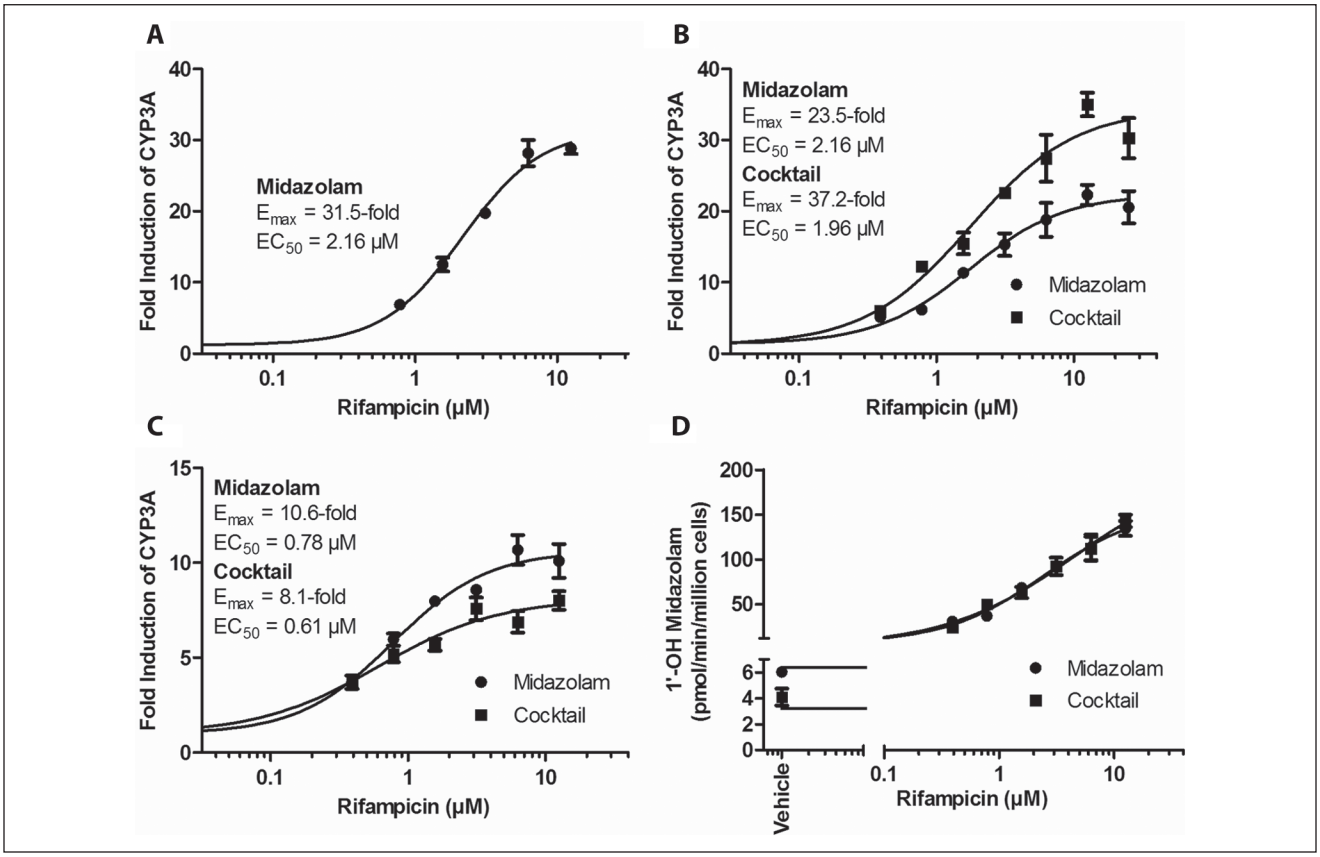


**Figure 1.** $EC_{50}/E_{max}$ determinations for rifampicin in a 24-well format with midazolam as the probe with lot 246 (**A**) and in a 96-well format comparing midazolam alone against a substrate cocktail with lots 246 (**B**) and 262 (**C**). (**D**) Activity versus concentration for rifampicin in a 96-well format comparing midazolam alone against a substrate cocktail with lot 246. Curve fitting required log transformation of concentrations, and a log transformation of 0 is not possible, so vehicle control was entered as $10^{-9}$ µM.

## *Assessment of Induction Potential for a Commercial Compound Set Using Four Concentrations*

To show the utility of this assay system, a group of 13 commercially available compounds, including known inducers and noninducers of CYPs, were tested at 0.3, 1, 10, and 30 µM in duplicate using lot 246 to replicate a scenario for high-throughput screening (HTS). The values for $EC_{50}$ and $E_{max}$ were estimated for compounds that induced greater than 1.5-fold for at least two concentrations and did not result in an ambiguous curve fit using three-parameter $EC_{50}$ and $E_{max}$ fittings. Estimated $EC_{50}$ and $E_{max}$ values were reported only if at least two tested concentrations were above the estimated $EC_{50}$ value. The baseline value of induction, with testing compound concentration at zero, was fixed to 1 to perform curve fittings resulting in the following equation:

$$\text{Fold induction} = 1 + \frac{E_{max} - 1}{1 + 10^{((\text{LogEC}_{50} - \text{Log[Compound]}) * \text{Hill slope})}}.$$

To allow comparison of compounds whose $E_{max}$ values were different, the concentrations to produce 2-, 3-, or 5-fold of induction ($EC_{x\text{-fold}}$) were calculated using fold induction values bracketing the target fold induction by the following formula:

$$EC_{x\text{-fold}} = [\text{Top}] - \frac{(\text{Top} - (\text{x-fold})) * ([\text{Top}] - [\text{Bottom}])}{\text{Top} - \text{Bottom}}.$$

The results for the commercial compound set are presented in **Table 6**.

$EC_{x\text{-fold}}$ values were calculated to allow more direct comparisons of induction potency between compounds. The calculation made the assumption of linearity in the estimated region. Despite the limitations of this simplified approach, the rank order of potency, as evidenced by the potency of typical positive controls such as rifampicin relative to other compounds, is demonstrated by these values.

CYP1A induction occurred with the two well-described inducers, β-naphthoflavone and omeprazole, but also

**Table 5.** Effect of Normalization by Cell Count on the Coefficient of Variation (%) for CYP Activities in 96-well

| | % CV without Normalization | | | | % CV with Normalization | | | |
|---|---|---|---|---|---|---|---|---|
| Treatment | CYP1A | CYP2B6 | CYP2C9 | CYP3A | CYP1A | CYP2B6 | CYP2C9 | CYP3A |
| | | | | **Lot 246, discrete probe** | | | | |
| Vehicle | 11.5 | 45.9 | 2.4 | 20.4 | 4.9 | 43.9 | 4.7 | 16.7 |
| β-NF 10 μM | 18.0 | — | — | — | 18.2 | — | — | — |
| PB 1 mM | — | 19.5 | — | — | — | 18.7 | — | — |
| Rif 10 μM | — | 14.3 | 10.6 | 4.4 | — | 16.4 | 16.0 | 10.9 |
| | | | | **Lot 246, cocktail probe** | | | | |
| Vehicle | 16.9 | 22.2 | 19.4 | 9.1 | 16.7 | 25.1 | 21.3 | 9.0 |
| β-NF 10 μM | 9.4 | 9.5 | 17.9 | 25.0 | 9.4 | 9.2 | 19.6 | 25.8 |
| PB 1 mM | 5.6 | 12.1 | 7.8 | 11.9 | 11.1 | 16.6 | 7.0 | 18.6 |
| Rif 10 μM | 7.5 | 11.4 | 17.4 | 3.5 | 9.0 | 16.6 | 20.8 | 2.4 |
| | | | | **Lot 262, discrete probe** | | | | |
| Vehicle | 8.7 | 13.6 | 8.6 | 13.0 | 8.7 | 7.3 | 7.9 | 7.8 |
| β-NF 10 μM | 1.8 | — | — | — | 1.6 | — | — | — |
| PB 1 mM | — | 26.7 | — | — | — | 17.5 | — | — |
| Rif 10 μM | — | 6.9 | 18.8 | 1.7 | — | 6.8 | 25.7 | 6.1 |
| | | | | **Lot 262, cocktail probe** | | | | |
| Vehicle | 17.6 | 40.0 | 20.8 | 16.3 | 15.0 | 40.3 | 19.9 | 13.9 |
| β-NF 10 μM | 7.3 | 7.1 | 15.6 | 3.9 | 1.9 | 9.5 | 19.3 | 1.6 |
| PB 1 mM | 4.8 | 12.6 | 20.6 | 8.1 | 8.6 | 11.9 | 23.4 | 9.7 |
| Rif 10 μM | 5.9 | 12.8 | 12.5 | 12.5 | 5.5 | 12.0 | 8.6 | 11.1 |
| **Mean of % CV** | 13.4 ± 8.7 | | | | 13.8 ± 8.7 | | | |

% coefficient of variation (CV) = SD/mean. —, not tested; β-NF, β-naphthoflavone; PB, phenobarbital; Rif, rifampicin.

occurred with rifampicin and troglitazone, which are known CYP3A inducers.[2,24,25] Rifampicin's estimated $EC_{50}$ value for increased CYP1A activity was similar to the value observed for its CYP3A induction, which suggests a possible link between the PXR signaling for CYP3A induction and the increase seen for CYP1A by treatment with rifampicin.

Many compounds induced CYP2B6, as expected, such as carbamazepine, phenytoin, and rifampicin.[2,26] Phenobarbital did not show significant induction at the concentrations tested, which is consistent with phenobarbital's reported $EC_{50}$ value of over 100 μM.[27] Again, β-naphthoflavone induced CYP2B6, and its $EC_{50}$ value was similar to the results obtained for CYP1A. This phenomenon may parallel rifampicin's apparent effect on CYP1A.

Weak induction by rifampicin was observed for CYP2C9, as previously reported.[2,28] In addition, lovastatin, omeprazole, and ritonavir appeared to weakly induce CYP2C9.

CYP3A was induced by many of the compounds in the panel, such as rifampicin and troglitazone.[29] Due to variability of the data at 0.3 μM for rifampicin and less data points to determine the curve, the $EC_{50}$ value does not match well with the full curve results from **Figure 1**. Ritonavir, a known PXR ligand and time-dependent inhibitor of CYP3A, showed no increase of CYP3A activity, which is consistent with ritonavir boosting the exposure of other human immunodeficiency virus (HIV) retrovirals by inhibiting CYP3A-mediated metabolism.[30]

The use of a substrate cocktail in a 96-well format with a form of cell counting is highly suitable for HTS for multiple reasons. By using the 96-well format and a substrate cocktail, the assessment of more compounds and more concentrations of those compounds can be accomplished without compromising the quality of the assessment. In addition, the use of a high-content screening system for counting the cells allows for a rapid in situ assessment of cell number and possible analysis of other cytotoxic parameters. That information from the high-content screening system allows for compensation of well-to-well variation and calculation of $EC_{50}$ values for cytotoxicity or other cytotoxic parameters due to compound treatment that could be used for evaluation of the induction data and ranking of potential hepatotoxicity of the compounds being screened. As a result, a substrate cocktail system, such as the one we have described, is a valuable tool in the rapid assessment of induction potential of drug candidates.

**Table 6.** Induction Potency of Various Commercial Compounds Assessed with Substrate Cocktail for CYP1A, CYP2B6, CYP2C9, and CYP3A: (**a**) Single Concentration Data and $EC_{50}$ and $E_{max}$ Values and (**b**) Estimated $EC_{x\text{-}fold}$ Values

| (**a**) | Carbamazepine | Clozapine | (±)-Ibuprofen | Lovastatin | Metoprolol | β-Naphthoflavone | Nevirapine | Omeprazole | Phenobarbital | Phenytoin | Rifampicin | Ritonavir | Troglitazone |
|---|---|---|---|---|---|---|---|---|---|---|---|---|---|
| | | | | | | **Fold induction** | | | | | | | |
| **CYP1A** | | | | | | | | | | | | | |
| 0.3 μM | 1.12 | 1.38 | 1.22 | 1.06 | 1.09 | 7.46 | 1.03 | 1.15 | 1.08 | 1.03 | 2.64 | 1.25 | 1.10 |
| 1 μM | 0.99 | 1.56 | 1.14 | 1.21 | 1.13 | 14.45 | 0.92 | 1.41 | 0.93 | 0.93 | 3.08 | 1.45 | 1.92 |
| 10 μM | 1.22 | 2.17 | 1.15 | 1.33 | 1.25 | 25.25 | 1.16 | 3.20 | 0.98 | 0.98 | 4.04 | 1.48 | 2.23 |
| 30 μM | 1.27 | 1.83 | 1.03 | 1.87 | 1.23 | 16.70 | 0.89 | 5.92 | 1.20 | 1.63 | 3.49 | 1.89 | 2.28 |
| $E_{max}$ (fold) | NC | 2.01 | NC | NC | NC | 20.94 | NC | NC | NC | NC | 3.80 | NC | 2.25 |
| $EC_{50}$ (μM) | NC | 0.60 | NC | NC | NC | 0.54 | NC | NC | NC | NC | 0.22 | NC | 0.70 |
| **CYP2B6** | | | | | | | | | | | | | |
| 0.3 μM | 1.27 | 1.52 | 1.36 | 0.54 | 1.36 | 2.06 | 1.00 | 1.26 | 1.33 | 1.68 | 3.14 | 1.86 | 1.31 |
| 1 μM | 1.23 | 1.83 | 1.33 | 0.54 | 1.25 | 2.27 | 1.04 | 1.37 | 1.08 | 2.58 | 6.81 | 3.76 | 2.57 |
| 10 μM | 2.77 | 3.31 | 1.53 | 1.28 | 1.76 | 3.87 | 2.37 | 2.54 | 1.47 | 6.20 | 12.35 | 3.84 | 5.97 |
| 30 μM | 3.65 | 1.99 | 1.48 | 3.47 | 1.61 | 4.41 | 2.29 | 4.16 | 2.21 | 6.71 | 9.53 | 2.86 | 9.17 |
| $E_{max}$ (fold) | NC | NC | NC | NC | NC | 6.51 | NC | NC | NC | 7.06 | 13.11 | 3.84 | NC |
| $EC_{50}$ (μM) | NC | NC | NC | NC | NC | 9.79 | NC | NC | NC | 2.30 | 1.07 | 0.38 | NC |
| **CYP2C9** | | | | | | | | | | | | | |
| 0.3 μM | 1.00 | 0.95 | 0.98 | 0.68 | 1.03 | 1.07 | 0.86 | 0.87 | 0.95 | 0.89 | 1.53 | 1.64 | 0.98 |
| 1 μM | 0.95 | 0.92 | 0.91 | 0.76 | 1.05 | 1.07 | 0.82 | 0.94 | 0.79 | 0.92 | 1.98 | 2.37 | 1.15 |
| 10 μM | 1.26 | 1.14 | 1.03 | 1.29 | 1.26 | 0.97 | 1.11 | 1.43 | 0.88 | 0.87 | 2.41 | 1.82 | 0.64 |
| 30 μM | 1.47 | 1.22 | 1.06 | 2.01 | 1.43 | 0.98 | 1.15 | 1.74 | 1.19 | 1.13 | 2.54 | 1.16 | 0.47 |
| $E_{max}$ (fold) | NC | NC | NC | NC | NC | NC | NC | NC | NC | NC | 2.55 | NC | NC |
| $EC_{50}$ (μM) | NC | NC | NC | NC | NC | NC | NC | NC | NC | NC | 0.60 | NC | NC |
| **CYP3A** | | | | | | | | | | | | | |
| 0.3 μM | 1.20 | 1.02 | 1.08 | 0.86 | 1.08 | 1.17 | 0.95 | 0.98 | 1.09 | 1.19 | 15.95 | 0.80 | 1.10 |
| 1 μM | 0.92 | 1.05 | 1.02 | 0.95 | 1.07 | 1.08 | 0.86 | 1.05 | 0.88 | 1.24 | 15.95 | 1.01 | 1.91 |
| 10 μM | 1.76 | 2.29 | 1.12 | 3.02 | 1.51 | 1.21 | 1.19 | 1.83 | 1.12 | 2.47 | 22.15 | 1.06 | 4.63 |
| 30 μM | 3.35 | 2.22 | 1.09 | 5.67 | 1.56 | 1.31 | 1.26 | 2.02 | 1.58 | 4.40 | 21.90 | 1.00 | 6.41 |
| $E_{max}$ (fold) | NC | NC | NC | NC | NC | NC | NC | 2.05 | NC | NC | 28.28 | NC | NC |
| $EC_{50}$ (μM) | NC | NC | NC | NC | NC | NC | NC | 4.92 | NC | NC | 0.23 | NC | NC |

*(continued)*

**Table 6.** (continued)

| (b) | Carbamazepine | Clozapine | (±)-Ibuprofen | Lovastatin | Metoprolol | β-Naphthoflavone | Nevirapine | Omeprazole | Phenobarbital | Phenytoin | Rifampicin | Ritonavir | Troglitazone |
|---|---|---|---|---|---|---|---|---|---|---|---|---|---|
| **CYP1A** | | | | | | **$EC_{x\text{-}fold}$ value (μM)** | | | | | | | |
| $EC_{2\text{-}fold}$ | NC | 7.49 | NC | NC | NC | 0.05 | NC | 3.97 | NC | NC | 0.18 | NC | 3.32 |
| $EC_{3\text{-}fold}$ | NC | NC | NC | NC | NC | 0.09 | NC | 8.99 | NC | NC | 0.87 | NC | NC |
| $EC_{5\text{-}fold}$ | NC | NC | NC | NC | NC | 0.19 | NC | 23.24 | NC | NC | NC | NC | NC |
| **CYP2B6** | | | | | | | | | | | | | |
| $EC_{2\text{-}fold}$ | 5.50 | 2.03 | NC | 16.58 | NC | 0.28 | 7.50 | 5.85 | 24.32 | 0.55 | 0.14 | 1.66 | 0.68 |
| $EC_{3\text{-}fold}$ | 15.23 | 8.11 | NC | 25.71 | NC | 5.11 | NC | 15.68 | NC | 2.04 | 0.28 | 6.40 | 2.14 |
| $EC_{5\text{-}fold}$ | NC | NC | NC | NC | NC | NC | NC | NC | NC | 7.02 | 0.65 | NC | 7.43 |
| **CYP2C9** | | | | | | | | | | | | | |
| $EC_{2\text{-}fold}$ | NC | NC | NC | 29.72 | NC | NC | NC | NC | NC | NC | 1.42 | 0.85 | NC |
| **CYP3A** | | | | | | | | | | | | | |
| $EC_{2\text{-}fold}$ | 13.02 | 7.90 | NC | 5.57 | NC | NC | NC | 27.89 | NC | 6.56 | 0.02 | NC | 1.30 |
| $EC_{3\text{-}fold}$ | 25.60 | NC | NC | 9.91 | NC | NC | NC | NC | NC | 15.49 | 0.04 | NC | 4.61 |
| $EC_{5\text{-}fold}$ | NC | NC | NC | 24.94 | NC | NC | NC | NC | NC | NC | 0.08 | NC | 14.16 |

n = 2. NC, not calculated.

## Acknowledgements

The authors thank Linda Buckley and Eric T. Williams (Eisai) for their editorial assistance and Eric for his thoughtful discussion of the work.

## Declaration of Conflicting Interests

The authors declared no potential conflicts of interest with respect to the research, authorship, and/or publication of this article.

## Funding

The authors were fully supported for the research and publication of this article by Eisai.

## References

1. Guengerich, F. P. Cytochrome p450 and Chemical Toxicology. *Chem. Res. Toxicol*. **2008**, *21*(1), 70–83.
2. Lin, J. H. CYP Induction-Mediated Drug Interactions: In Vitro Assessment and Clinical Implications. *Pharm. Res*. **2006**, *23*(6), 1089–1116.
3. Hardwick, J. P.; Gonzalez, F. J.; Kasper, C. B. Transcriptional Regulation of Rat Liver Epoxide Hydratase, NADPH–Cytochrome P-450 Oxidoreductase, and Cytochrome P-450b Genes by Phenobarbital. *J. Biol. Chem*. **1983**, *258*(13), 8081–8085.
4. Parsons, W. D.; Neims, A. H. Effect of Smoking on Caffeine Clearance. *Clin. Pharmacol. Ther*. **1978**, *24*(1), 40–45.
5. Li, A. P.; Reith, M. K.; Rasmussen, A.; Gorski, J. C.; Hall, S. D.; Xu, L.; Kaminski, D. L.; Cheng, L. K. Primary Human Hepatocytes as a Tool for the Evaluation of Structure-Activity Relationship in Cytochrome P450 Induction Potential of Xenobiotics: Evaluation of Rifampin, Rifapentine and Rifabutin. *Chem. Biol. Interact*. **1997**, *107*(1–2), 17–30.
6. Sueyoshi, T.; Negishi, M. Phenobarbital Response Elements of Cytochrome P450 Genes and Nuclear Receptors. *Annu. Rev. Pharmacol. Toxicol*. **2001**, *41*, 123–143.
7. Chen, S.; Wang, K.; Wan, Y. J. Retinoids Activate RXR/CAR-Mediated Pathway and Induce CYP3A. *Biochem. Pharmacol*. **2010**, *79*(2), 270–276.
8. Pelkonen, O.; Turpeinen, M.; Hakkola, J.; Honkakoski, P.; Hukkanen, J.; Raunio, H. Inhibition and Induction of Human Cytochrome P450 Enzymes: Current Status. *Arch. Toxicol*. **2008**, *82*(10), 667–715.
9. Chu, V.; Einolf, H. J.; Evers, R.; Kumar, G.; Moore, D.; Ripp, S.; Silva, J.; Sinha, V.; Sinz, M.; Skerjanec, A. In Vitro and In Vivo Induction of Cytochrome p450: A Survey of the Current Practices and Recommendations: A Pharmaceutical Research and Manufacturers of America Perspective. *Drug Metab. Dispos*. **2009**, *37*(7), 1339–1354.
10. Fahmi, O. A.; Kish, M.; Boldt, S.; Obach, R. S. Cytochrome P450 3A4 mRNA Is a More Reliable Marker Than CYP3A4 Activity for Detecting Pregnane X Receptor–Activated Induction of Drug-Metabolizing Enzymes. *Drug Metab. Dispos*. **2010**, *38*(9), 1605–1611.
11. Mugundu, G. M.; Hariparsad, N.; Desai, P. B. Impact of Ritonavir, Atazanavir and Their Combination on the CYP3A4 Induction Potential of Efavirenz in Primary Human Hepatocytes. *Drug Metab. Lett*. **2010**, *4*(1), 45–50.
12. Walsky, R. L.; Obach, R. S. Validated Assays for Human Cytochrome P450 Activities. *Drug Metab. Dispos*. **2004**, *32*(6), 647–660.
13. Feidt, D. M.; Klein, K.; Hofmann, U.; Riedmaier, S.; Knobeloch, D.; Thasler, W. E.; Weiss, T. S.; Schwab, M.; Zanger, U. M. Profiling Induction of Cytochrome p450 Enzyme Activity by Statins Using a New Liquid Chromatography–Tandem Mass Spectrometry Cocktail Assay in Human Hepatocytes. *Drug Metab. Dispos*. **2010**, *38*(9), 1589–1597.
14. Lahoz, A.; Donato, M. T.; Picazo, L.; Castell, J. V.; Gómez-Lechón, M. J. Assessment of Cytochrome P450 Induction in Human Hepatocytes Using the Cocktail Strategy plus Liquid Chromatography Tandem Mass Spectrometry. *Drug Metab. Lett*. **2008**, *2*(3), 205–209.
15. Rhodes, S. P.; Otten, J. N.; Hingorani, G. P.; Hartley, D. P.; Franklin, R. B. Simultaneous Assessment of Cytochrome P450 Activity in Cultured Human Hepatocytes for Compound-Mediated Induction of CYP3A4, CYP2B6, and CYP1A2. *J. Pharmacol. Toxicol. Methods* **2011**, *63*(3), 223–226.
16. Cawley, G. F.; Batie, C. J.; Backes, W. L. Substrate-Dependent Competition of Different P450 Isozymes for Limiting NADPH–Cytochrome P450 Reductase. *Biochemistry* **1995**, *34*(4), 1244–1247.
17. Nishimura, M.; Koeda, A.; Suganuma, Y.; Suzuki, E.; Shimizu, T.; Nakayama, M.; Satoh, T.; Narimatsu, S.; Naito, S. Comparison of Inducibility of CYP1A and CYP3A mRNAs by Prototypical Inducers in Primary Cultures of Human, Cynomolgus Monkey, and Rat Hepatocytes. *Drug Metab. Pharmacokinet*. **2007**, *22*(3), 178–186.
18. Maglich, J. M.; Stoltz, C. M.; Goodwin, B.; Hawkins-Brown, D.; Moore, J. T.; Kliewer, S. A. Nuclear Pregnane X Receptor and Constitutive Androstane Receptor Regulate Overlapping but Distinct Sets of Genes Involved in Xenobiotic Detoxification. *Mol. Pharmacol*. **2002**, *62*(3), 638–646.
19. Wang, H.; Li, H.; Moore, L. B.; Johnson, M. D.; Maglich, J. M.; Goodwin, B.; Ittoop, O. R.; Wisely, B.; Creech, K.; Parks, D. J.; et al. The Phytoestrogen Coumestrol Is a Naturally Occurring Antagonist of the Human Pregnane X Receptor. *Mol. Endocrinol*. **2008**, *22*(4), 838–857.
20. Lim, Y. P.; Kuo, S. C.; Lai, M. L.; Huang, J. D. Inhibition of CYP3A4 Expression by Ketoconazole Is Mediated by the Disruption of Pregnane X Receptor, Steroid Receptor Coactivator-1, and Hepatocyte Nuclear Factor 4alpha Interaction. *Pharmacogenet. Genomics* **2009**, *19*(1), 11–24.
21. Zhou, C.; Poulton, E. J.; Grün, F.; Bammler, T. K.; Blumberg, B.; Thummel, K. E.; Eaton, D. L. The Dietary Isothiocyanate Sulforaphane Is an Antagonist of the Human Steroid and Xenobiotic Nuclear Receptor. *Mol. Pharmacol*. **2007**, *71*(1), 220–229.

22. Podvinec, M.; Handschin, C.; Looser, R.; Meyer, U. A. Identification of the Xenosensors Regulating Human 5-Aminolevulinate Synthase. *Proc. Natl. Acad. Sci. U. S. A*. **2004**, *101*(24), 9127–9132.
23. Ulbrichova, D.; Hrdinka, M.; Saudek, V.; Martasek, P. Acute Intermittent Porphyria—Impact of Mutations Found in the Hydroxymethylbilane Synthase Gene on Biochemical and Enzymatic Protein Properties. *FEBS J*. **2009**, *276*(7), 2106–2115.
24. Curi-Pedrosa, R.; Daujat, M.; Pichard, L.; Ourlin, J. C.; Clair, P.; Gervot, L.; Lesca, P.; Domergue, J.; Joyeux, H.; Fourtanier, G. Omeprazole and Lansoprazole Are Mixed Inducers of CYP1A and CYP3A in Human Hepatocytes in Primary Culture. *J. Pharmacol. Exp. Ther*. **1994**, *269*(1), 384–392.
25. Ramachandran, V.; Kostrubsky, V. E.; Komoroski, B. J.; Zhang, S.; Dorko, K.; Esplen, J. E.; Strom, S. C.; Venkataramanan, R. Troglitazone Increases Cytochrome P-450 3A Protein and Activity in Primary Cultures of Human Hepatocytes. *Drug Metab. Dispos*. **1999**, *27*(10), 1194–1199.
26. Pelkonen, O.; Myllynen, P.; Taavitsainen, P.; Boobis, A. R.; Watts, P.; Lake, B. G.; Price, R. J.; Renwick, A. B.; Gómez-Lechón, M. J.; Castell, J. V.; et al. Carbamazepine: A 'Blind' Assessment of CVP-Associated Metabolism and Interactions in Human Liver-Derived In Vitro Systems. *Xenobiotica* **2001**, *31*(6), 321–343.
27. Hariparsad, N.; Carr, B. A.; Evers, R.; Chu, X. Comparison of Immortalized Fa2N-4 cells and Human Hepatocytes as In Vitro Models for Cytochrome P450 Induction. *Drug Metab. Dispos*. **2008**, *36*(6), 1046–1055.
28. Sahi, J.; Shord, S. S.; Lindley, C.; Ferguson, S.; LeCluyse, E. L. Regulation of Cytochrome P450 2C9 Expression in Primary Cultures of Human Hepatocytes. *J. Biochem. Mol. Toxicol*. **2009**, *23*(1), 43–58.
29. Luo, G.; Cunningham, M.; Kim, S.; Burn, T.; Lin, J.; Sinz, M.; Hamilton, G.; Rizzo, C.; Jolley, S.; Gilbert, D.; et al. CYP3A4 Induction by Drugs: Correlation between a Pregnane X Receptor Reporter Gene Assay and CYP3A4 Expression in Human Hepatocytes. *Drug Metab. Dispos*. **2002**, *30*(7), 795–804.
30. Hull, M. W.; Montaner, J. S. Ritonavir-Boosted Protease Inhibitors in HIV Therapy. *Ann. Med*. **2011**, *43*(5), 375–388.